

BIOMECHANICAL AND BIOLOGICAL PROPERTIES OF CRYOPRESERVED CANINE AMNIOTIC
MEMBRANE



A Thesis Submitted in Partial Fulfillment of the Requirements
for the Degree of Master of Science in Veterinary Surgery
Department of Veterinary Surgery
Faculty of Veterinary Science
Chulalongkorn University
Academic Year 2018
Copyright of Chulalongkorn University

คุณสมบัติทางชีวกลศาสตร์และชีววิทยาของเยื่อหุ้มตัวอ่อนสุนัขที่เก็บถนอมด้วยวิธีการแช่แข็ง



วิทยานิพนธ์นี้เป็นส่วนหนึ่งของการศึกษาตามหลักสูตรปริญญาวิทยาศาสตรมหาบัณฑิต

สาขาวิชาสัตวศาสตร์ทางสัตวแพทย์ ภาควิชาสัตวศาสตร์

คณะสัตวแพทยศาสตร์ จุฬาลงกรณ์มหาวิทยาลัย

ปีการศึกษา 2561

ลิขสิทธิ์ของจุฬาลงกรณ์มหาวิทยาลัย

5975302131 : MAJOR VETERINARY SURGERY

KEYWORD: AMNIOTIC MEMBRANE, BIOLOGY, BIOMECHANICS, CANINE,
CRYOPRESERVATION

Nathawan Withavatpongton : BIOMECHANICAL AND BIOLOGICAL
PROPERTIES OF CRYOPRESERVED CANINE AMNIOTIC MEMBRANE. Advisor:
Asst. Prof. Dr. NALINEE TUNTIVANICH, D.V.M., M.S., Ph.D.

Amniotic membrane (AM) is the innermost fetal membrane. Due to its many known properties, human AM is a favorable corneal graft. Cryopreservation at -80°C maintains most of biological properties. Due to shortage of supply, AM of other species are studied. The objective of this study is to explore the biomechanical and biological properties of canine AM (CAM) after cryopreservation for 7 and 30 days. CAMs were collected from healthy bitches undergoing cesarean sections. After preservation, they were tested for tensile strength by Universal Testing Machine, transparency by spectrophotometer, sterility by microbial culture, cell viability by trypan blue staining, and histological study by Hematoxylin/eosin and Masson Trichrome stain. J-shaped stress-strain curve was produced on all samples. Maximum stress, extensibility, and Young's modulus were not statistically different. Transparency and haze were not significantly different. Some bacteria and fungi were identified on both groups. Cell viability of 7-day CAMs was significantly higher than 30-day CAMs. Collagen was found in stromal layer. The stroma of 30-day CAM was significantly flattened. This research showed that cryopreservation for 30 days did not significantly affect biomechanical properties, and only partially affect biological properties. It is suggested that cryopreserved CAM has promising properties suitable for clinical use as corneal graft.

Field of Study: Veterinary Surgery

Student's Signature

Academic Year: 2018

Advisor's Signature

ACKNOWLEDGEMENTS

First, this study would not have been possible without my kind advisor Asst. Prof. Nalinee Tuntivanich. I especially am grateful for her support, encouragement, and guidance.

I thank the thesis committees Assistant Professor Kumpanart Soontornvipart, Professor Emeritus Pranee Tuntivanich, Associate Professor Anudep Rangsipipat, and Associate Professor Pinnita Tanthuvanit for their valuable suggestions to fulfill this thesis.

I most appreciate the help and equipment support from Division of Obstetrics, Gynaecology and Reproduction, Division of Pathology, Division of Biochemistry, Faculty of Veterinary Science, Chulalongkorn university, Oncology Clinic, and Ophthalmology unit, Small Animal Teaching Hospital on collection, processing, cryopreservation and histological processing of canine amniotic membrane. I also appreciate assistance and equipment service from the Dental Material Science Center, Faculty of Dentistry, Chulalongkorn University.

This study was financially funded by Graduate Student Fund, Faculty of Veterinary Science, Chulalongkorn University, and 90th Anniversary of Chulalongkorn University Scholarship.

Finally, this research would not have been possible without my beloved parents, family and friends' endless love, understanding, and support.

Nathawan Withavatpongton

TABLE OF CONTENTS

	Page
.....	iii
ABSTRACT (THAI).....	iii
.....	iv
ABSTRACT (ENGLISH).....	iv
ACKNOWLEDGEMENTS.....	v
TABLE OF CONTENTS.....	vi
LIST OF TABLES.....	ix
LIST OF FIGURES.....	x
CHAPTER 1 INTRODUCTION.....	1
Importance and Rationale.....	1
Research Questions.....	2
Objectives.....	2
Advantages of Study.....	3
CHAPTER 2 LITERATURE REVIEW.....	4
Anatomy of the Eye.....	4
Cornea.....	4
Corneal Ulcer.....	7
Corneal Healing.....	8
Treatment of Corneal Ulcers.....	9
Corneal Perforation.....	9
Corneal Grafts.....	10

Amniotic Membrane.....	10
Canine amniotic membrane	13
Amniotic Membrane Preparations.....	15
Biomechanical Properties of Amniotic Membrane	17
Tensile Strength Test	17
Transparency Test	19
Biological Properties of Amniotic Membrane.....	20
Sterility	20
Viability	20
Histology.....	21
CHAPTER 3 MATERIALS AND METHODS	23
Materials.....	23
Canine Amniotic Membranes	23
Media	23
Methods.....	24
Sample Collection.....	24
Cryopreservation.....	25
Part 1: Biomechanical Properties of Canine Amniotic Membrane.....	26
Tensile Strength Test	26
Transparency Test	28
Part 2: Biological properties of Canine Amniotic Membrane.....	30
Sterility Test.....	30
Cell viability Test	30
Histological Test.....	32

Data Analysis.....	33
CHAPTER 4 RESULTS.....	36
Part 1: Biomechanical Properties of Canine Amniotic Membrane.....	36
Tensile Strength Test	36
Transparency Test	37
Part 2: Biological Properties of Canine Amniotic Membrane	38
Sterility Test.....	38
Cell Viability Test.....	39
Histological Test.....	40
CHAPTER 5 DISCUSSION	43
Conclusion.....	46
Suggestions.....	46
REFERENCES	47
APPENDIX.....	54
Part 1: General data of included canine amniotic membranes	54
Part 2: Biomechanical data of canine amniotic membranes.....	54
Part 3: Biological data of canine amniotic membranes	57
VITA.....	63

LIST OF TABLES

	Page
Table 1: Median \pm interquartile range of tensile strength parameters of canine amniotic membranes cryopreserved at 7 and 30 days.....	37
Table 2: Median \pm interquartile range of transparency parameters of canine amniotic membranes cryopreserved at 7 and 30 days.....	37
Table 3: Median \pm interquartile range of canine amniotic membranes cryopreserved at 7 and 30 days. Note: Star (*) indicates statistical difference.	42
Table 4: Tensile strength test results of 7-day CAMs	54
Table 5: Tensile strength test results of 30-day CAMs.....	55
Table 6: Transparency test results of 7-day CAMs	56
Table 7: Transparency test results of 30-day CAMs.....	57
Table 8: Microbial culture results of 7-day CAMs.....	57
Table 9: Microbial culture results of 30-day CAMs.....	58
Table 10: Cell viability results of 7-day CAMs.....	59
Table 11: Cell viability results of 30-day CAMs.....	60
Table 12: Histological measurement results of 7-day CAMs.....	61
Table 13: Histological measurement results of 30-day CAMs.....	61

LIST OF FIGURES

	Page
Figure 1: Cross section diagram of canine eyeball	4
Figure 2: Corresponding (A) micrograph (Magg et al., 2017) and (B) diagram of cornea layers.....	5
Figure 3: Schematic illustrations of (A) anatomy of canine placenta and (B) histology of CAM.	15
Figure 4: Schematic illustration of J-shaped stress-strain curve and their associated collagen fiber morphology	19
Figure 5: Photograph of CAM collection materials.....	24
Figure 6: Photograph of CAM (A) after washing and (B) cutting to size with nitrocellulose membranes attached.....	25
Figure 7: A storage vial of CAM for biological test. (Note the clear label and secure lid).....	26
Figure 8: (A) A schematic diagram illustrating how CAM sample was mounted on the UTM's grip with a nitrocellulose paper cut in the opposite direction of the pulling force. Photographs of (B) CAM readily mounted on UTM's grip and (C) CAM being pulled in a vertical direction.....	27
Figure 9: Illustration of a J-shaped stress-strain curve typically found in a biological material and tensile strength values derived from the curve. Note: stress at fracture point = max stress, strain at fracture point = extensibility.....	28
Figure 10: (A) Schematic diagram corresponding to (B) a photograph of CAM mounted apparatus for transparency test.....	29
Figure 11: Schematic illustration of light transmission through a medium for transparency test.....	29

Figure 12: Photographs of (A) a side view and (B) a front view of a spectrophotometer (Ultrascan Pro, HunterLAB, USA) with its cover removed with a sample mounted apparatus in measuring position.....	30
Figure 13: A schematic diagram of the 3x2 cm ² CAM for (A) cell viability test and (B) histological test.....	31
Figure 14: Photograph of CAM after it was mounted on microscopic slide and stained with trypan blue.	31
Figure 15: Photographs of (A) CAMs in cassettes fixed in formalin and (B) cassettes with CAMs during embedding to paraffin block.....	33
Figure 16: Photograph of microscope connected to a digital camera that was used to take microphotographs of CAM samples.....	33
Figure 17: Representative stress-strain curves of (A) 7-d and (B) 30-d canine amniotic membrane. (Note: MPa = Megapascal).....	36
Figure 18 : Pie charts of bacterial culture from (A) 7-d CAM and (B) 30-d CAM samples. (Note that numbers indicate number of positive samples.)	38
Figure 19: Pie charts of fungal culture from (A) 7-d CAM and (B) 30-d CAM samples. (Note that numbers indicate number of positive samples.)	39
Figure 20: Representative microphotographs showing single layer of epithelium of (A) 7-d CAMs and (B) 30-d CAMs, comprising of nonviable (Trypan blue stained) cells and viable cells (Trypan blue unstained) (arrows). (bar = 100 micron)	40
Figure 21: Bar chart of the Median \pm interquartile range of percentage of cell viability of cryopreserved amniotic membranes at 7 and 30 days. Note: Star (*) indicates statistical difference.	40
Figure 22: Representative microphotographs of the 7-day canine amniotic membrane stained with (A) Hematoxylin and Eosin (H&E) and (B) Masson Trichrome (MTS), and the 30-day canine amniotic membrane stained with (C) H&E and (D) MTC. Note that arrows indicate fibroblasts within the stromal layer while an arrow head indicates cilia sloughing off from epithelial layer. (magnification power = 400X, bar = 25 micron)...	41



จุฬาลงกรณ์มหาวิทยาลัย
CHULALONGKORN UNIVERSITY

CHAPTER 1

INTRODUCTION

Importance and Rationale

Corneal ulceration is one of the most common ocular diseases in veterinary ophthalmology. It is caused from various etiologies; trauma, ocular abnormalities or infections. If left untreated, corneal ulceration can progress to severe complications including descemetocoele, corneal perforation, anterior staphyloma and ultimately the loss of vision. Prompt and precise treatments of corneal ulcers are required. Correction of the primary cause, control of infection, stimulation of corneal healing process, together with the minimization of inflammation and limitation of self-trauma are key factors. In deep stromal corneal ulcers, surgical reconstruction provides strength of corneal integrity. Amniotic membrane (AM) has played an important role as a biomaterial for corneal reconstruction. AM derived from various species such as humans (Tuntivanich and Tuntivanich, 2006) equine (Ollivier et al., 2006), bovine (Kim et al., 2009), porcine (Tsuzuki et al., 2008) and canine (Barros et al., 2005) are clinically reported.

As human amniotic membrane (HAM) has become clinically widespread, its low availability of tissue harvest and the health risks associated with fresh tissue (Laranjo, 2015) are major concern. Preservation and sterilization methods are invented to maintain the AM's most competent biomechanical and biological properties as to the fresh material, whilst ensuring the safety of the recipient (Nakamura et al., 2004; Riau et al., 2010). It has been proven that cryopreservation can preserve HAM most important properties at near-fresh qualities (Laranjo, 2015). For the most beneficial outcome many important factors that have been concerned include tensile strength (von Versen-Hoeynck et al., 2008), transparency (Connon et al., 2010), antimicrobial properties (Mao et al., 2017), lack of immunogenicity (Jirsova

and Jones, 2017), epithelial promotion and loss of cell viability after preservation (Hennerbichler et al., 2007).

Biomechanical properties of a transplanted material are important for surgeons to predict intra-and post-operative behavior of grafting materials (Chuck et al., 2004). Several biomechanical properties are affected by methods of preservation (von Versen-Hoeynck et al., 2008; Hariya et al., 2016). Amniotic membrane generates a J-shaped stress-strain curve of tensile strength, which is typically found in soft tissue biological materials (Holzapfel, 2001; Borazjani et al., 2011). Materials with such stress-strain curve shape can withstand some deformation without breaking, which is a desirable trait for a grafting material.

There is increasing incidence of corneal damage in companion animals. While clinical request of AM graft is currently raised, material supply is insufficient. According to a few reports of successful clinical usage of CAM for corneal reconstruction in animals (Barros et al., 2005; Kalpravidh et al., 2009; Vongsakul et al., 2009), it is suggested that CAM is an effective grafting material as to AM from other species. Up to present, details of biomechanical and biological properties of CAM have never been characterized.

Research Questions

1. Are biomechanical properties of cryopreserved CAM significantly different between preservation time at 7 and 30 days?
2. Are biological properties of cryopreserved CAM significantly different between preservation time at 7 and 30 days?

Objectives

1. To compare biomechanical properties of CAM after 7 and 30 days of cryopreservation
2. To compare biological properties of CAM after 7 and 30 days of cryopreservation

Advantages of Study

Novel and detailed knowledge of biomechanical and biological properties of CAM after 7 and 30 days of cryopreservation allows further development of preservation methods for CAM to be efficiently used for clinical corneal reconstruction in animals.



CHAPTER 2

LITERATURE REVIEW

Anatomy of the Eye

From superficial to deep, the globe consists of the following: the fibrous outer layer consisting of the cornea and the sclera, the blood vessel rich middle layer called the uvea consisting of iris, ciliary body, and choroid, and the inner retina which is where the photoreceptors are located. The chambers inside are divided to aqueous chamber and vitreous chamber. The aqueous chamber is filled with aqueous humor and can be subdivided to the anterior and posterior chamber by the iris. The vitreous chamber is filled with gelatinous-like vitreous body that maintains the shape of the globe (Maggs et al., 2017) (Figure 1).

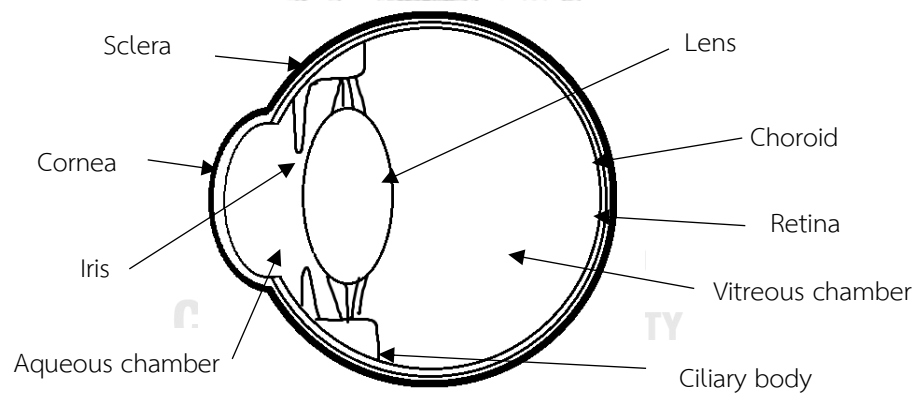


Figure 1: Cross section diagram of canine eyeball

Cornea

The fibrous outermost layer of the globe consists of the transparent cornea and the opaque sclera. They make up the structure and shape of the eye. The anterior part of the sclera is covered with translucent conjunctiva. The circular area

that the sclera, cornea, and the conjunctiva connect is called the limbus. The cornea's curved and smooth surface combined with the tear film provide an excellent light refraction material. Its shape is circular or slightly horizontally oval when viewed from the front (Maggs et al., 2017). The thickness varies between species. For dogs, the mean corneal thickness is 631.07 ± 59.91 micron (Wolfel et al., 2019).

The cornea consists of 5 layers; the epithelium, the basement membrane, the stroma, the Descemet's membrane, and the endothelium (Figure 2).

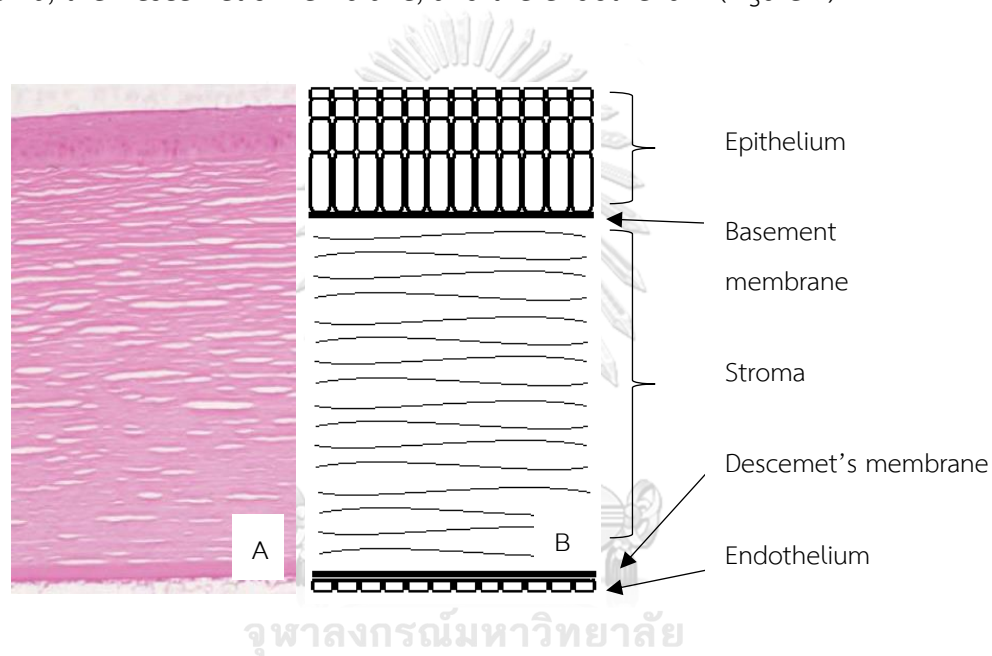


Figure 2: Corresponding (A) micrograph (Maggs et al., 2017) and (B) diagram of cornea layers.

Corneal epithelium is stratified squamous non-keratinized type. In dogs and cats, they consist of 6-7 layers of cells. From the basement membrane to superficial, the deepest basal cell layer is columnar in shape, the middle layer is polyhedral (wing cells), and the surface layer is flat (squamous). The basal layer is attached to the basement membrane by hemidesmosomes. As the basal cells divide and migrate to the surface, the daughter cells gradually lose its shape and organelles. At the surface level, they develop microvilli which hold the tear film to the corneal surface.

The basal cells are replaced by daughter cells that are divided from limbal stem cells and migrate towards the center; therefore, corneal cells regeneration and maturation occur simultaneously and constantly throughout life (Maggs et al., 2017).

Basement membrane is secreted by the epithelial cells. It is composed of collagen type IV, VII, laminin, fibronectin, nidogen, perlecan and other proteins (Gonzalez-Andrades et al., 2019). They provide anchoring hemidesmosomes for the corneal epithelial cells to adhere to.

Corneal stroma is composed of keratocytes, collagen, glycosaminoglycan, and other ground substances that can be found in extracellular matrix. The stroma makes up 90% of the cornea's thickness and provides the cornea's rigidity which contributes to the globe's structural stability. The collagen within this layer is constructed in parallel layers of interlacing sheets with interspersed cells such as keratocytes, lymphocytes, macrophages, and neutrophils. The cornea's transparency is maintained by this regular structure. If this structure is disturbed by any inclusion, such as water (edema), scar tissue, or over infiltration of cells, the transparency is lost.

Descemet's membrane is the basement membrane of the endothelium. It is constantly renewed by secretion of the endothelial cells and thus it becomes thicker with age. This membrane is elastic. However, it could break if put under high pressure as found in glaucoma (Haab's striae), or by penetrating injuries (ruptured cornea). In case of deep corneal ulcer in which the entire stromal layer was lost, the Descemet's membrane can become exposed. This is called "Descemetocele". It appears to be dark but transparent, cannot be stained by fluorescein, and may bulge forward out of the corneal ulcer by intraocular pressure.

Endothelium is a single layer of cells lining the anterior part of the aqueous chamber. It pumps ions from the stroma to aqueous, and by extension, water. This causes the stroma to remain relatively dehydrated and keeps the cornea transparent by maintaining the parallel structure of collagen sheets. The endothelial cells in adult animals have limited ability to divide and therefore can become decreased in

number as the animal age. It is a common finding in geriatric animals that the cornea becomes thicker from slight edema. The normal density of endothelial cells in young dogs is 2800 cell/mm², when the cell count decreases below 500-800 cell/mm², the cornea loses its ability to adequately pump water out of the stroma. Edema that is caused by loss of endothelial cells is permanent. The endothelium can also be damaged by trauma, surgery, inflammation, and glaucoma.

There is no blood vessel, melanin, or keratin on the cornea, in combination with low cell density, regular structure of stromal collagen sheets, and the smooth surface provided by the pre-corneal tear film, the cornea's transparency is maintained. Disruption of these properties will decrease the transparency of the cornea. It can be caused by edema, scar, infiltration of cells, pigments, vascularization, tear film instability and many other causes.

Due to lack of blood vessels, the cornea receives oxygen and nutrients from atmosphere, tear film, adjacent conjunctival capillaries, and aqueous humor (Maggs et al., 2017).

Corneal Ulcer

Corneal ulceration is defined by the disruption or loss of an entire corneal epithelium with or without involvement of the stroma. Physiologically, the epithelium is constantly abraded by normal blinking and replaced with new cells migrated from the limbus at a balanced rate. If imbalanced, epithelial cell loss is excessive while cell renewal is deficient, corneal ulcer occurs. In superficial non-complicated corneal ulcer, healing process should not take longer than 7 days. If the lesion is deep and the duration is prolonged, then it is classified as complicated ulcer (Groth et al., 2015). Vision can be impaired. Corneal ulcers can become infected. The most common pathogens on canine and feline corneas are *Staphylococcus aureus*, *Streptococcus β-hemolyticus* and *Pseudomonas aeruginosa* (Ollivier, 2003). In case of deep ulcers, surgical intervention by corneal reconstruction should be performed to prevent risk of corneal perforation and other possible sequelae; such as corneal melting, uveitis, and ultimately blindness. Corneal reconstruction is a procedure to

correct corneal integrity, corneal transparency, volume of anterior chamber and visual function. With this procedure, vision can be restored in an otherwise blinding injury. In order to reestablish corneal integrity, biological transplants are suggested.

Corneal Healing

The epithelium has excellent healing capability. The adjacent cells to the damaged area start migrating to the lesion within the first few minutes. As the cells move towards the central area of the cornea, the melanocytes from the limbus can move along. The affected area should be covered with new epithelial cells within 4-7 days, followed by cell mitosis to reestablish multilayer structure of the epithelium. Finally, the attachment of hemidesmosome to the basement membrane occurs.

The stroma heals by two mechanisms; vascular healing and avascular healing. Vascular healing mechanism is often found in uncomplicated ulcers, while the other is often found in complicated ulcers. The stromal healing process can take years to fill the space completely; therefore, a stromal defect can be found in case of deeper ulcers that has already completed its epithelial healing process. In avascular healing, neutrophils from tear, aqueous humor, and limbal blood vessels migrate to surround the lesion. The keratocytes from surrounding area migrate to replace the dead keratocytes in the lesion, transform to fibroblast, and secrete collagen, mucoprotein, and glycosaminoglycans. The collagen secreted is not regularly arranged and therefore; the transparency decreases. The macrophages migrate into the lesion to remove cell debris within 48 hours. Scar resolution can take months, the scar fades but never completely disappear, and the degree of scar resolution varies between age and species of the affected animal. The vascular healing occurs with the neovascularization extending from the limbal vessels. Cellular infiltration is increased, granular tissue is formed, and the scar left behind is denser. After the healing process was completed, the new blood vessels become constricted. The non-perfused blood vessels can be seen with slit lamp and are called “ghost vessels”.

The Descemet's membrane can be regenerated by the endothelial cells' secretion. However, the endothelial cells themselves have limited regeneration

capability especially in mature animals. Extensive loss of endothelial cells can cause permanent corneal edema.

Treatment of Corneal Ulcers

The most important treatment for any ulcer is to identify and correct the underlying cause. Topical antibiotics is prescribed along with prevention of self-trauma. In cases of uncomplicated ulcer, the lesion should resolve in 7 days. If not, then the diagnosis is changed to complicated ulcer and treatment must be changed as such. In deep ulcers, the treatment is more extensive than those of uncomplicated ones. Along with removal of underlying cause and antibiotics, mydriatic drugs and protease inhibitors should be used. Because of devastating nature of corneal melting that may occur by infection, deep ulcers are assumed to be infected unless proven otherwise. Protease inhibitors that are often used are acetylcysteine and autologous serum. Because of slower regeneration capability of the corneal stroma, surgical treatment is beneficial to deep ulcers. It is recommended unless the animal is not a candidate for surgery.

The most common surgical treatment for corneal ulcers includes protection and mechanical support of cornea by third eyelid flap. However, in case of deeper ulcers to perforation, corneal suturing may be required. In case of large lesions, a replacement material for the loss of corneal integrity may be needed.

Corneal Perforation

Corneal perforation is a corneal injury that penetrate every layer of the cornea. If left untreated, the globe can lose its shape from loss of aqueous humor. Goals of treatment are to seal the leak and restore integrity of the cornea (Maggs et al., 2017). Bandage contact lens is a non-invasive choice for small corneal perforations. It can promote epithelial healing and reduce pain (Rodriguez-Ares et al., 2004). Other methods to correct integrity include third-eyelid flaps, conjunctival flap, and tarsorrhaphy. These methods provide stability and blood vessels, but aqueous humor leakage can still occur from pressuring the eyeball. Tissue adhesive had been

studied to be used as corneal sealant. It can promptly restore integrity to the globe in cases of small perforation without infection. However, dislodging of adhesive can cause the lesion to become bigger (Duchesne et al., 2001). Corneal suturing is another effective way to seal a small leakage on cornea, however, it can cause astigmatism, which is a concern especially in humans. In larger perforations, corneal grafts from other materials are recommended (Maggs et al., 2017).

Corneal Grafts

There are several materials that are acceptable to use as corneal graft such as conjunctiva, (Groth et al., 2015), small intestinal submucosa (Bussieres et al., 2004), urinary bladder submucosa (Davis et al., 2017), pericardium (Dulaurent et al., 2014), amniotic membrane (Tuntivanich and Tuntivanich, 2006; Brikshavana and Kanchanachaya, 2010), and cornea (Lacerda et al., 2017). The conjunctiva is easily available and is an effective graft to reestablish corneal integrity and provide blood vessels that supplies nutrients and systemic drugs to the lesion. However, its opacity and its heavy scarring after healing can reduce vision to the eye. This limitation causes several studies to be conducted on other materials that may be used in its stead. Cornea is the best material for this purpose. However, corneal graft's supply is extremely insufficient. Thus, other materials that can be substitute to the corneal graft is always in high demand.

Amniotic Membrane

Amniotic membrane is the innermost layer of the fetal membrane that is devoid of vasculature. It consists of a single layer of epithelium, basement membrane and a thick stroma, which is subdivided to three layers; compact, fibroblast and spongy. In humans, amniotic membrane attaches to the chorion membrane by its stromal side. HAM is histologically 0.02-0.5 mm thick (Jirsova and Jones, 2017). Epithelial layer contains one layer of cuboidal cells with villi, which are arranged uniformly. This layer is attached firmly to the basement membrane. The basement membrane is made up of collagen fibers types IV, V, VI, fibronectin, and laminin (Iranpour et al., 2018). It supports epithelial cell attachment and cell

proliferation without cytotoxic effects (Iranpour et al., 2018). Amniotic membrane epithelium has extracellular matrix component identical to that of the conjunctiva (Fukuda et al., 1999). Stromal layer contains abundance of collagen fibers types I, II, III, IV, and V, as well as a lot of other proteins including fibronectin, laminins and hyaluronic acid (Jirsova and Jones, 2017). During pregnancy, amnion holds most of the physical force on the fetal membrane. It has been demonstrated that the amniotic membrane can withstand more force than the chorion despite being thinner. Interestingly, the chorioamnion as a bilayer can hold more force than the two membranes when measured separately (Verbruggen et al., 2017). The compact layer of HAM stroma is the strongest part among all layers due to its compact collagen structure (Riau et al., 2010). Transparency varies among different regions; the proximal region next to placenta is slightly less transparent than the distal region (Connon et al., 2010).

HAM can act as anatomical and vapor barrier making it an effective moisture holding bandage that can promote healing. HAM epithelial cells are multipotent cell that can differentiate to many types of cells (Laranjo, 2015). It is known that HAM produces various growth factors including epidermal growth factor, basic fibroblast growth factor, hepatocyte growth factor and keratinocyte growth factors. The basement membrane of the HAM promotes migration, proliferation, and adhesion of epithelial cells and prevents apoptosis (Iranpour et al., 2018). Presence of bacticidin, beta-lysin, lysozyme, transferrin and 7-S immunoglobulins in amniotic fluid (Mao et al., 2017) and defensin in the membrane (Jirsova and Jones, 2017) suggests antibacterial property of HAM. Moreover, HAM demonstrates its beneficial characteristics of having anti-inflammatory properties by inhibiting of pro-inflammatory cytokines (Marsh et al., 2017), anti-fibrotic activity by inhibiting the expression of transforming growth factor that activates fibroblast activity (Rihardini et al., 2017), anti-angiogenic effect by producing thrombospondin1, endostatin and tissue inhibitors of metalloproteases (Hao et al., 2000) and lack of immunogenicity (Jirsova and Jones, 2017).

Various methods are invented to preserve amniotic membrane properties for transplantation; such as air-dried, freeze-dried, cryopreserved and cold glycerol preserved. Since bacterial contamination had been reported on both HAM that were delivered by cesarean section and vaginally, sterilization is a mandatory process (Addis et al., 2001). After being kept at room temperature overnight and sterilized by irradiation, air-dried HAM increases its tensile strength (von Versen-Hoeynck et al., 2008) and shelf life up to 5 years (Singh and Chacharkar, 2011). However, the thickness, amount of growth factors, and ability to be cultivated with human limbal epithelial cells are decreased (Jirsova and Jones, 2017). Air-dried HAM that is sterilized by gamma radiation less than 20 kGy may have resulted in significant changes of morphological and structural properties of the membrane. Decomposition of collagen and a reduction of growth factors are also reported (Mrázová et al., 2016). Preservation by freeze drying, or lyophilization, is performed by rapidly freezing of HAM and removing its water content to less than 10%. Freeze-dried HAM decreases in thickness, cell viability, and amount of growth factors, compared to cryopreserved HAM. Storage of cold glycerol preserved HAM at -20°C up to 6 weeks has not had clinically significant difference as compared to the cryopreserved one (Ashraf et al., 2015).

The most seemingly used preservation method is cryopreservation. This method is first developed by Tseng and colleagues (Tseng, 2007). The storage media usually consists of 1:1 glycerol and Dulbecco's Modified Eagle's Medium (DMEM). The most common antimicrobial cocktail is penicillin/streptomycin/ neomycin, and amphotericin B (Jirsova and Jones, 2017). HAM undergone cryopreservation results in better thickness, remaining of basement membrane components and growth factors and ability to be cultivated by epithelial cells, in comparison to other preservation methods (Jirsova and Jones, 2017).

Depending on purpose of transplantation, clinical application of cryopreserved HAM includes inlay (grafting) and overlay (patching) technique. For inlay technique, HAM is attached to corneal lesion with its epithelial side up. The membrane provides itself as a scaffold for new epithelial cells to grow on. While the

overlay technique is used for the purpose of having the new epithelial cells grow underneath the transplant. The membrane is placed with the epithelial side either up or down. To increase strength of the membrane for transplantation, application of multilayer can be considered (Jirsova and Jones, 2017). Clinical corneal reconstructions with the use of HAM are reported; ocular surface disorder (Barros et al., 2005), corneal perforations, descemetocoele, deep ulcers (Berguiga et al., 2013), corneal neoplasia (Espana et al., 2002), chemical and thermal burns of the cornea (Prabhasawat et al., 2007), bullous keratopathy (Espana et al., 2003), infectious corneal ulcer (Barequet et al., 2008), reduction of corneal haze after laser photoablation (Wang et al., 2001), and persistent corneal epithelial defects (Dekaris et al., 2010). In veterinary practice, clinical use of HAM is reported in cats with corneal sequestrum (Barachetti et al., 2010) and dogs with severe corneal damage (Brikshavana and Kanchanachaya, 2010).

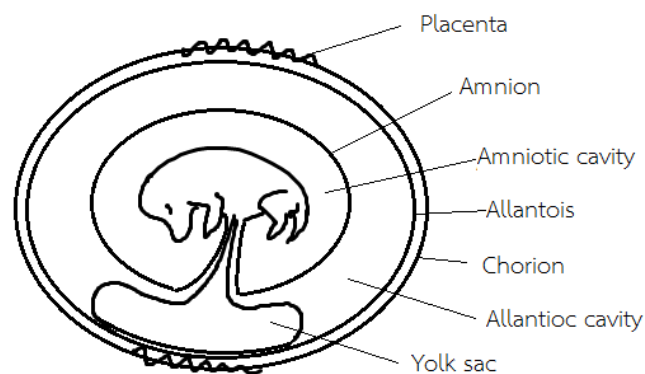
Canine amniotic membrane

The CAM, like the human counterpart, is composed of epithelium, basement membrane and stroma. However, there are anatomical differences. Canine placenta is in zonary form, while the human placenta is discoid. In humans, amniotic membrane is attached to the chorion and the membrane remains avascular to term. In canine, on the other hand, amnion and chorion are not attached. With allantois blood vessels formation at the later stage of pregnancy, CAM slightly becomes vascularized near the umbilical cord (Miglino et al., 2006). On the last day of pregnancy, CAM becomes the thickest and evident with the cuboidal epithelial cell arrangement (Aralla et al., 2013).

Corneal reconstruction with the use of CAM is conducted in many cases; keratomalacia, ankyloblepharon and corneal histiocytoma in dogs and cat (Barros et al., 2005), corneal dermoid (Kalpravidh et al., 2009) and created deep corneal ulcers (Vongsakul et al., 2009). Following reconstructive surgery to repair the cornea, an increase epithelialization without scar formation or neovascularization is noted. This suggests that CAM can be used clinically as an effective corneal grafting material, and

that it may have anti-inflammatory, anti-angiogenic and anti-fibrotic properties similar to those of HAM (Hao et al., 2000).

Though fresh and cryopreserved HAM are clinically as effective as the cornea for transplantation, cell viability is different. There is no evident of proliferative ability in a long-term preserved HAM, while some degree of cell viability remains after short term preservation (Jirsova and Jones, 2017). Cell viability has 13-18% reduction after being cryopreserved for 3 weeks (Hennerbichler et al., 2007). However, some loss of cell viability might be considered beneficial as to a low-grade inflammatory response of tissue (John, 2003). Despite the fact that there is a difference in terms of cell viability, cryopreserved HAM reveals comparable sterility, histological and biological properties to the fresh membrane after a long-term preservation up to 24 months (Thomasen et al., 2011). Its tensile strength shows a stress-strain curve typical of an elastic material with toe region. By means of using CAM as an alternative grafting material, details knowledge of biomechanical and biological properties of preserved CAM should be investigated.



A

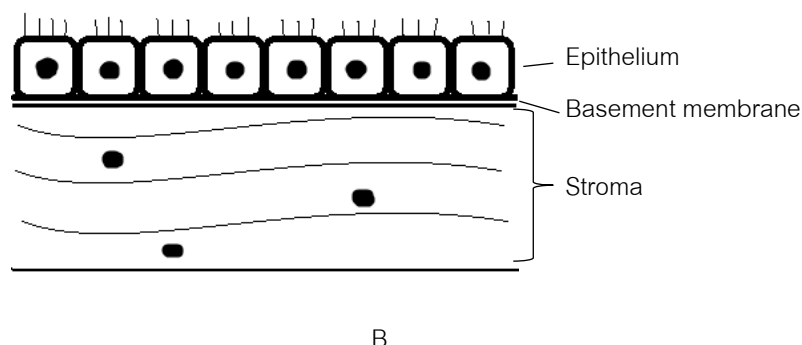


Figure 3: Schematic illustrations of (A) anatomy of canine placenta and (B) histology of CAM.

Amniotic Membrane Preparations

Fresh AM may retain all its beneficial properties, but there is potential risk of infection. Thus, prolonged preservation time is mandatory for various tests to be carried out. Because bacterial culture test typically takes 5-7 days to complete and report, AM must be kept preserved for at least 1 week to be used safely (Lagier et al., 2015). There are many ways of collection and preservation of AM, all with their own benefits and limitations.

There are several methods to collect AM. Usually collected AM is processed in laminar flow hood, washed with sterile saline combined with antibiotics cocktail against gram positive and negative bacteria and fungi. In HAM, the chorion must be bluntly dissected from the AM before the AM is cut to size and stored in individual sterile vials and quarantined until serology tests are available (Dua et al., 2004). In CAM, the AM is not attached to the chorion (Figure 3).

Cryopreservation in glycerol: DMEM (1:1) at -80°C is the preservation method recommended by Food and Drug Administration and is the most used method for long term preservation (Laranjo, 2015; Jirsova and Jones, 2017). This method can keep HAM usable with near-fresh quality and preserve most of the beneficial properties for several months, up to 2 years (Dua et al., 2004). However, cryopreservation alone is not known for sterilization ability. Bacteria and viruses are

found to be viable after several months of cryopreservation (Riau et al., 2010). Glycerol dehydrates the AM without osmotic alteration, acting as a cryoprotectant. Several tests, such as vital staining, ultrastructural analysis, and cell culture, were done to test cell viability of cryopreserved AM. It is found that the epithelial cells typically do not survive the process. This can be considered an advantage due to non-viable cells produce less immunogenicity. The limitation of this method is that it requires a laboratory-graded ultra-freezer, which is often not available in clinical setting, and is difficult to transport (Riau et al., 2010; Laranjo, 2015). There are reports of AM cryopreservation in other media such as in Dimethyl sulfoxide (DMSO) with satisfactory clinical results. However, studies of its structural integrity and biological contents are not yet available (Riau et al., 2010). The purpose of DMSO cryopreservation at this point is mostly for experiments aiming for higher cell viability (Jirsova and Jones, 2017). It has been reported that 50% of cells were proliferative after cryopreservation in DMSO for 2 months, but not after 18 months (Kubo et al., 2001).

Lyophilization or freeze-drying is removal of water by sublimation. This method causes some of the structure to become permanently changed, which also stops deterioration from occurring. Therefore, it can be stored at room temperature in a long term, which may reduce the cost of storage when compared to cryopreservation (Laranjo, 2015). After storing in vacuum, this method is often combined with gamma-ray irradiation for sterilization. Gamma radiation is an effective sterilization method against several bacteria, viruses and fungi. There are reports of gamma radiation affecting tissue integrity. Lyophilized AM appears to be thinner than cryopreserved AM. It also has similar tensile strength, and lower growth factor content than cryopreserved AM (Riau et al., 2010). There are reports of successful use of lyophilized AM for corneal graft in rabbits (Riau et al., 2010).

Air-dried AM is prepared by flattening washed AM and letting it dry overnight in a laminar flow cabinet. This procedure removes water from the tissue, resulting in tissue that can be kept in room temperature in a long term. Its simpler procedure and lower cost make air-drying an interesting method. However, it's been shown that

some properties of AM are lost by this method of preservation. It is mostly used for wound dressing with effective results (Singh and Chacharkar, 2011).

Cross-linking HAM with chemical method or radiation method can improve tensile strength and transparency. This procedure also lowers degradation rate by enzymatic digestion. It can be done by glutaraldehyde, gamma radiation, or electron beam. Multilayered HAM undergone cross-linking process is more resilient than cryopreserved HAM (Laranjo, 2015; Hariya et al., 2016). It is reported to be an effective corneal graft material that can maintain limbal cell culture both *in vitro* and *in vivo* (Laranjo, 2015).

To reduce disease transmission risk, many sterilization methods are developed. Ionizing radiation such as gamma radiation is an effective method used in many medical products. Its penetrative properties and low heat production make it suitable for pre-packaged materials, and thus it is often used in combination with lyophilized AM. It eliminates bacteria, viruses, and fungi. However, some biological and biomechanical properties are affected by this method (Riau et al., 2010). Chemical sterilization by paracetic acid is reported to be an effective method to eliminate bacteria, viruses, and fungi. This method is considered safe to use in biomaterials since paracetic acid breaks down to non-toxic residues, namely, acetic acid and oxygen peroxide. The structures of AM, especially basement membrane components, are satisfactory preserved. Tensile strength and elasticity are not significantly affected by this method. *In vitro* tests on limbal cell culture on paracetic sterilized AM reported that similar morphology and proliferation rate. However, clinical uses of AM that are sterilized by paracetic acid are not yet reported (Laranjo, 2015).

Biomechanical Properties of Amniotic Membrane

Tensile Strength Test

Tensile strength is one of the mechanical properties than can be tested on engineering material. Its purpose is to test deformation rate to pulling force applied

to the material. By mounting the material to Universal Testing Machine, the force exerted (load) can be recorded at a constant interval of time as the material is pulled apart at a constant rate. The graph that is generated is called the load-elongation graph. The data can be further calculated to find the stress (load divided by area), and strain (length changed divided by original length). The relationship between stress and strain can be displayed by the stress-strain curve, which is unique to each material (Holzapfel, 2001).

There are 3 possible shapes for stress-strain curve. The linear (Hookean), concave non-linear (J-shaped), and convex non-linear (r-shaped). The linear curve is often found in engineering materials such as metal. The J-shaped curve is found in biological materials such as skin or amniotic membrane (Holzapfel, 2001) (Figure 4), and the r-shaped curves are found in rubber (Berthoume, 2016).

The limitation of this test is it assumes the material is homogeneous in every direction. However, it is often not the case in biological materials, since they often are heterogenous and directionally dependent. While it may be more scientifically appropriate to measure each component individually, it is useful to test the estimated mechanical properties of the entire system as a single item (Holzapfel, 2001).

Studies done on AM have found that the AM's stress-strain curve matches those of the J-shape type due to their collagen and elastin-rich stroma. Elastin is a protein with multiple cross-linking bond with itself and has high elasticity properties. The initial phase of pulling did not pull on the collagen fiber, but on elastin's cross-linking bond, which makes the first phase of elongation requires low stress. Preservation and sterilization methods may affect tensile strength of AM, as air-dried HAM had been demonstrated to have higher tensile strength than cryopreserved HAM (von Versen-Hoeynck et al., 2008). Dry preparations demonstrated higher Young's modulus than moist preparations. Sterilization by electron beam irradiation gives HAM more stiffness whereas the required force to rupture is decreased (Chuck et al., 2004). Cross-linking multiple layers of HAM also gives the resulting material

higher tensile strength (Hariya et al., 2016). Species that have AM with the highest loading are the equine and human, and the species that present the highest elasticity are porcine and ovine (Borazjani et al., 2011) Due to biomechanical properties of AM may influence clinical applications, these data are valuable. Up to date, there has not been reports on the tensile strength of CAM.

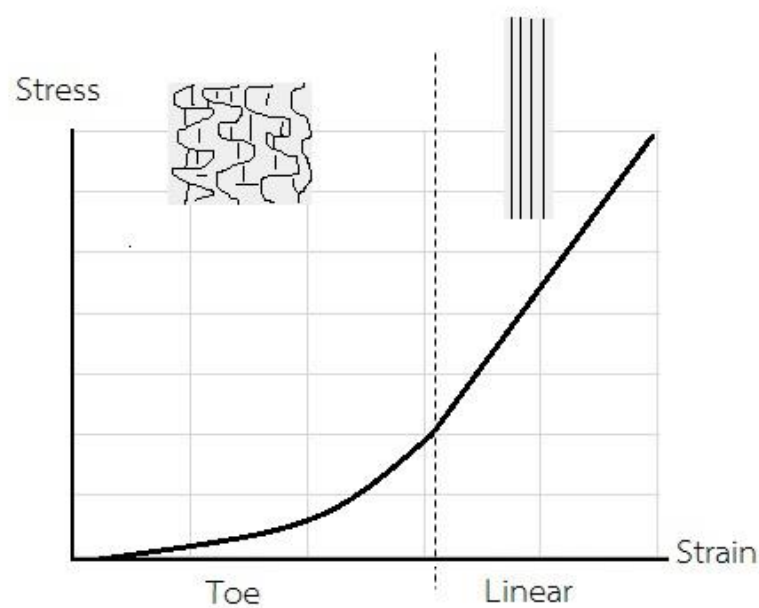


Figure 4: Schematic illustration of J-shaped stress-strain curve and their associated collagen fiber morphology

Transparency Test **CHULALONGKORN UNIVERSITY**

There are not many studies done on AM's quantitative transparency. A study had shown that HAM's transparency is affected by preparation method. Freeze-dried AM is shown to be more transparent than cryopreserved HAM. However, transparency negatively correlates to thickness. (Connon et al., 2010). Multilayered HAM undergone cross-linking results in higher transparency, as compared to those without cross-linking process (Hariya et al., 2016). Up to date, there has not been reports on CAM's transparency.

Biological Properties of Amniotic Membrane

Sterility

Bacterial growth is reported in samples of HAM collected by vaginal delivery and cesarean section after aseptically collected and incubated at 37°C for 1 week (Addis et al., 2001). Cryopreservation on its own is not a guaranteed way of sterilization as viruses and bacteria are found to be viable after several months (Riau et al., 2010). However, it has been demonstrated that HAM has antibacterial properties in varying degree depending on bacterial strains. This property is shown to not be affected by cryopreservation and freeze-drying (Tehrani et al., 2013). Up to date, there has not been reports on CAM's sterility or antimicrobial properties.

Viability

In the majority of preservation methods, such as cryopreservation in glycerol, lyophilization, and air-drying, cell viability of the AM is significantly lost. There are some methods that can maintain cell viability such as cryopreservation in DMSO and fresh preservation at 4°C. Studies on temperature and storage condition on cell viability of HAM demonstrated that HAM that are kept at 4°C in glycerol/DMEM result in immediate cell death. HAM that are kept in DMEM at 37°C remain 45% viable after storing for 28 days. HAM kept in Leibovitz's L15-medium in either room temperature or at 4°C remain 15-35% viable. Cryopreservation result in significant reduction of viability with no influence of preservation media (Hennerbichler et al., 2007). Important properties of HAM are from the matrix as the scaffold, not by cell proliferation (Dua et al., 2004). Cell viability may increase immunogenicity, but it might be beneficial in other context such as research, or skin wound healing (Laranjo, 2015).

Histology

Normal histology of HAM consists of epithelial layer, basement membrane, and stromal layer. The stromal layer can be subdivided to compact layer and spongy layer. CAM histology differs from HAM. CAM is demonstrated to be thinner, epithelial cells are shown to be ciliated, and the stromal layer are not obviously subdivided (Favaron et al., 2015). Different preservation methods affect histological morphology of HAM differently. Maintenance of basement membrane and stromal matrix of HAM is crucial to promote epithelialization. Cryopreservation maintains HAM structure similar to fresh, while air-drying causes major structural changes, such as condensation of microvilli and intercellular channels sterilization by radiation can damage internal structure. Air-dried AM has more sensitivity to radiation damage than cryopreserved AM in glycerol. Macroscopically, lyophilization causes the membrane to become thinner and more fragile. Histologically, the important features HAM, especially the basement membrane, remains intact. Some areas of epithelial layers are shown to be lost by lyophilization. Vacuolar degeneration and flattening of epithelial cells are also found on lyophilized HAM. Cryopreservation may produce some vacuolar degeneration and stromal edema. Acid pretreatment and air-drying result in complete loss of biological properties of HAM. Decellularized-dehydrated HAM has severe alteration in its basement membrane structure, with loss of collagen type IV, V, fibronectin, laminin and growth factors (Laranjo, 2015). Currently, no studies of effects of preservation on CAM histological morphology are reported.

CHAPTER 3

MATERIALS AND METHODS

Materials

Canine Amniotic Membranes

Thirty-six samples of CAM from healthy puppies were collected from pregnant bitches. All bitches were 1-6 years of age. They underwent Caesarean section at the Small Animal Teaching Hospital, Faculty of Veterinary Science, Chulalongkorn University. All bitches had completed vaccination program. Collection of CAM were performed under aseptic technique, followed by instantaneous preservation. Exclusion criteria included history of systemic infection or inflammation of reproductive system within 3 months prior to surgery. Bitches with history of abortion or dead fetus, current abortion or dead fetus, high white blood cell count at pre-anesthesia or signs of inflammation of amniotic membrane were excluded.

Media

Equipment and bottles were sterilized by autoclave. Preparation of solutions were done in a laminar flow hood.

Washing solution: A 0.01 M phosphate buffer solution (PBS) was prepared by mixing PBS tablet (Gibthai, Thailand) into 1 liter of deionized water. The solution was autoclaved, then 1 ml of 5-5-10 mg/ml Penicillin-Streptomycin-Neomycin antibiotic mixture (PSN) (Gibthai, Thailand) and 0.5 ml of 5 mg/ml Amphotericin B (Gibthai, Thailand) were added into the solution in a laminar flow hood. The solution was thoroughly mixed before use.

Storage solution: Storage solution was prepared in a laminar flow hood on the day of sample collection. Glycerol in Dulbecco modified Eagle medium (DMEM)

at 1:1 ratio was prepared by mixing 50 ml of pre-autoclaved glycerol (ChemEx, India) and 50 ml of DMEM (Gibthai, Thailand), then 1 ml of PSN and 0.02 ml of Amphotericin B were added into the mixture. After the solution was thoroughly mixed, it was transferred to one 30-ml glass vial and two 20-ml glass vials for each individual sample. All glass vials were pre-autoclaved and kept securely lidded in a temperature insulator box with an ice pack until use.

Methods

Sample Collection

Sample collection was performed with sterile technique in a surgical unit. Before Cesarean section, a collection tray was prepared by lining the tray with gauze and then filling it with a sterile solution (Figure 5). Extra gauzes were prepared on a sterile area for extra samples within the same surgery. Following a removal of a puppy from the uterus, fetal membrane was peeled off. CAM was immediately spread into a sheet with its epithelial side up onto the prepared collection tray. The sample was covered with another sheet of spread gauze, then the next sample was collected in the same way. To keep CAM fresh and clean, collection tray was securely lidded and placed into a temperature insulator box with ice pack, then immediately transported to a laminar flow hood.



Figure 5: Photograph of CAM collection materials.

Cryopreservation

In a laminar flow hood, CAM was washed multiple times with washing solution to remove visible blood clots and staining. CAM was then transferred to another tray and washed again at least 3 times on each side or until the used solution was transparent. The selective non-vascularized part of each membrane was attached by their stromal side to 3 different sizes of autoclaved nitrocellulose membranes; 5x2, 4x4, and 3x2 cm². CAM was cut to size, and securely wrapped onto the attached nitrocellulose membranes (Figure 6). They were submerged separately into storage solution in 30 ml vial, 20 vial and 20 ml vial respectively (Figure 7). Lids were securely closed before they were removed from laminar flow hood. All vials were clearly labeled and transported in temperature insulator box with ice packs and randomly cryopreserved at -80°C for 7 days (7-d CAM; n=18), and 30 days (30-d CAM; n=18).



Figure 6: Photograph of CAM (A) after washing and (B) cutting to size with nitrocellulose membranes attached.

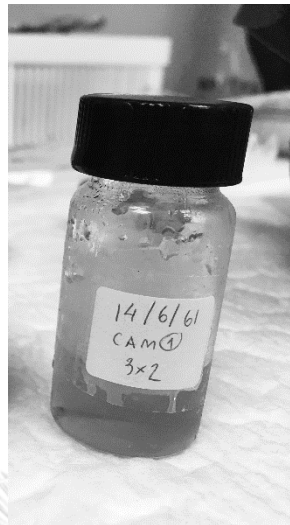


Figure 7: A storage vial of CAM for biological test. (Note the clear label and secure lid)

The study was divided into 2 parts:

Part 1: Study of biomechanical properties of CAM

Part 2: Study of biological properties of CAM

Part 1: Biomechanical Properties of Canine Amniotic Membrane Tensile Strength Test

After their respective cryopreservation time, the 5x2 cm² CAM was assigned for the tensile strength test. The test was performed with a Universal Testing Machine (UTM; Shimadzu, Japan). After the membrane was thawed from -80°C, the membrane, still attached to nitrocellulose membrane, was gently washed several times with washing solution. The membrane was then mounted by securing the upper and the lower clamp, at 1 cm on both sides of the membrane. After the membrane was fixed onto the UTM's grip (Figure 8), nitrocellulose paper was cut across in the middle of the strip horizontally. Tensile strength test was performed

automatically by a tensile testing computerized program (Trapezium 2, Shimadzu, Japan). The program was set to pull the membrane apart vertically at the rate of 5 mm/min, the pulling force was measured and recorded every 0.05 seconds until fracture.

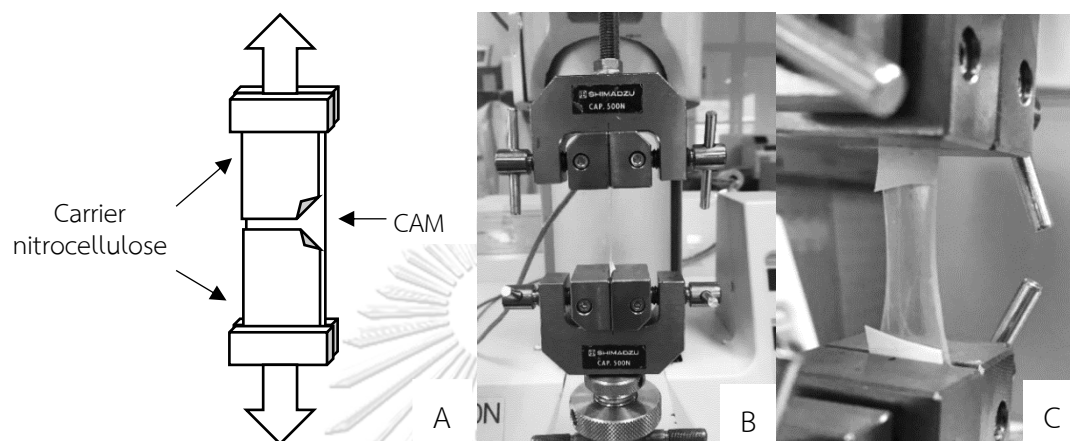


Figure 8: (A) A schematic diagram illustrating how CAM sample was mounted on the UTM's grip with a nitrocellulose paper cut in the opposite direction of the pulling force. Photographs of (B) CAM readily mounted on UTM's grip and (C) CAM being pulled in a vertical direction.

The stress-strain curve was automatically generated by the software (Trapezium 2 Shimadzu, Japan,). As CAM was a biological material, the curve was expected to be J-shaped type. The toe region was defined by the concave area at the beginning of the graph, which was followed by the linear region at the end of the curve (Figure 9). The experiment ended at fracture point, where the membrane completely or partially broke. The values that were reported in this study were maximum stress (Megapascal, MPa), extensibility (no unit), Young's modulus (MPa), length of toe region (no unit), and length of linear region (no unit). Young's modulus constant is calculated from the slope of the stress-strain curve at the linear part by this equation;

$$\text{Young's modulus} = \text{Stress} / \text{Strain}$$

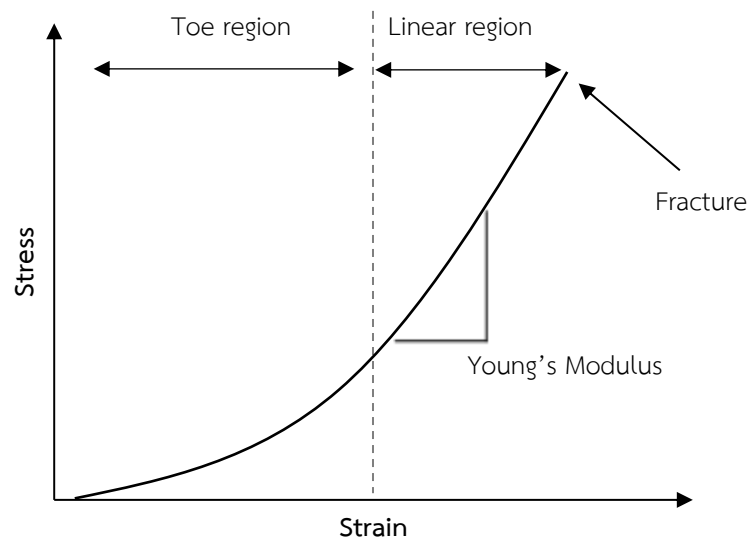


Figure 9: Illustration of a J-shaped stress-strain curve typically found in a biological material and tensile strength values derived from the curve. Note: stress at fracture point = max stress, strain at fracture point = extensibility

Transparency Test

After cryopreservation for their respective time, the 4x4 cm² CAM was assigned for the transparency test. The test was performed with the use of a spectrophotometer (Ultrascan Pro, HunterLAB, USA). After the membrane was thawed from -80°C, the membrane wrapped on the nitrocellulose paper was gently washed several times with washing solution until the membrane became loosen from the nitrocellulose paper. The unwrapped membrane was mounted between two pieces of Kraft paper that had a 3-cm diameter circular cut-out hole (Figure 10). The sample mounted apparatus was loaded onto the transmission compartment of the spectrophotometer (Figure 12). Quantitative measurement of light that can pass through the membrane (transmitted light) and diffuse light (haze) was automatically performed using total transmittance (TTRAN) mode of the software (EasyMatch QC ver 4.88.03, HunterLAB, USA).

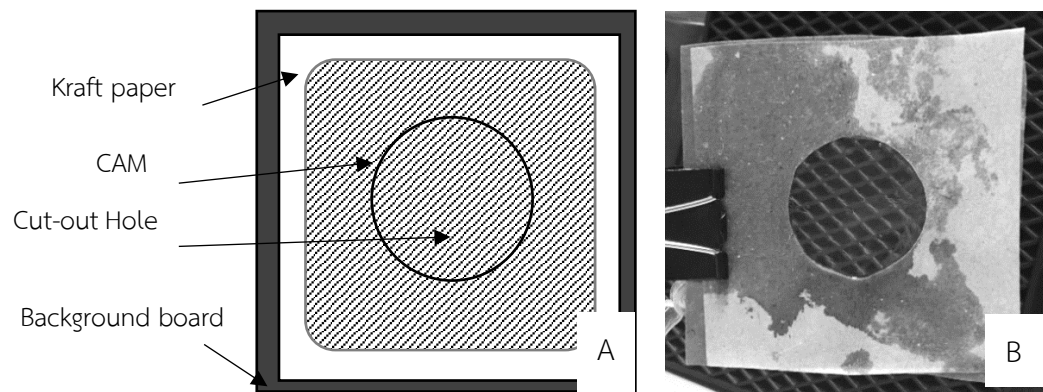


Figure 10: (A) Schematic diagram corresponding to (B) a photograph of CAM mounted apparatus for transparency test.

Result of transparency test was reported as percentage of TTRAN (%TTRAN) and percentage of Haze (%Haze). Definition of %TTRAN was the percentage of TTRAN to incident light, and %Haze was the percentage of diffusely transmitted light to TTRAN (Figure 11). %TTRAN and %Haze were automatically calculated by these equations;

$$\%TTRAN = \frac{\text{Directly transmitted light} + \text{diffusely transmitted light} \times 100}{\text{Incident light}}$$

$$\%Haze = \frac{\text{Diffusely transmitted light}}{\text{Directly transmitted light} + \text{diffusely transmitted light}} \times 100$$

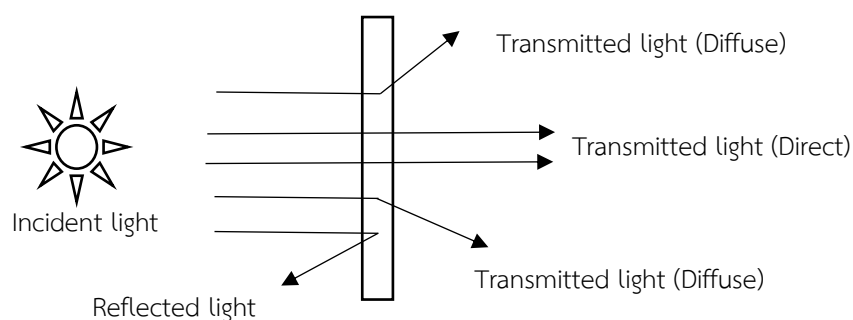


Figure 11: Schematic illustration of light transmission through a medium for transparency test.

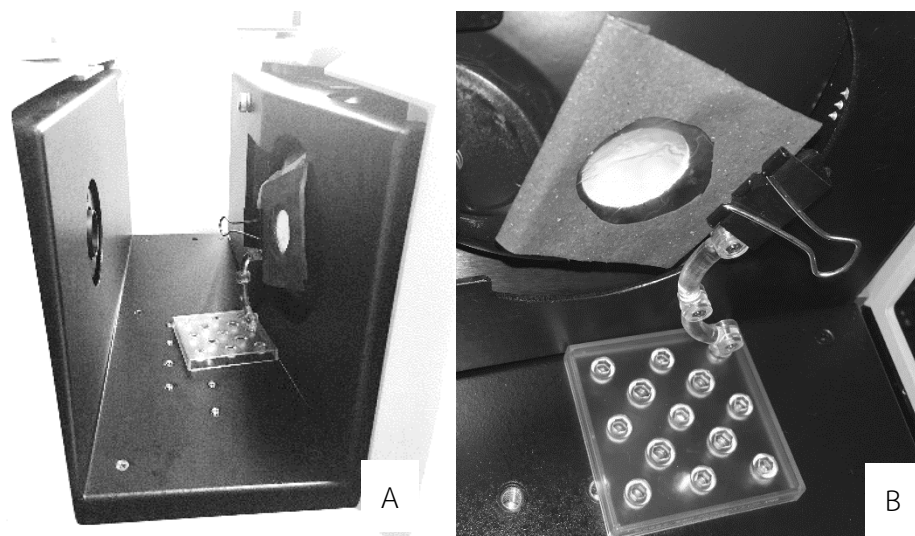


Figure 12: Photographs of (A) a side view and (B) a front view of a spectrophotometer (Ultrascan Pro, HunterLAB, USA) with its cover removed with a sample mounted apparatus in measuring position.

Part 2: Biological properties of Canine Amniotic Membrane

Sterility Test

Storage solution of the $3 \times 2 \text{ cm}^2$ CAM after cryopreserved for its respective time was collected after it was thawed from -80°C . A sterile swab was dipped into the storage solution before being placed into a transport media. The tube was submitted for culture and identification of bacteria and fungus.

Cell viability Test

After the $3 \times 2 \text{ cm}^2$ CAM that was cryopreserved for its respective time was thawed from -80°C , it was gently washed with washing solution and cut in $2 \times 2 \text{ cm}^2$ piece (A) and $2 \times 1 \text{ cm}^2$ piece (B) (Figure 13).

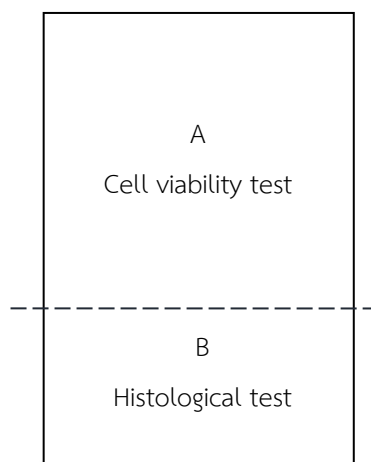


Figure 13: A schematic diagram of the 3x2 cm² CAM for (A) cell viability test and (B) histological test.

Sample A (Figure 13) was used for cell viability test by modified trypan blue dye exclusion staining. The sample was gently washed with washing solution then mounted on a microscopic slide with its epithelium side up (figure 14). 20 microliter of trypan blue was added onto the sample. The sample was incubated for 3 minutes before washing off with washing solution. The sample was visualized under light microscope.

จุฬาลงกรณ์มหาวิทยาลัย
CHULALONGKORN UNIVERSITY

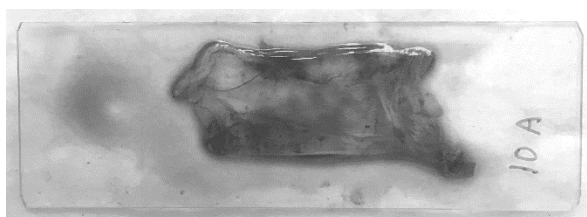


Figure 14: Photograph of CAM after it was mounted on microscopic slide and stained with trypan blue.

Five different fields of microphotographs were randomly taken for each sample; percentage of viable cells was averaged by manually counting stained and

un-stained cells in microphotographs. This test result was described by percentage of viable cells (%viable) compared to all cells. The equation for viable cell percentage was as follows;

$$\%Viable = \frac{\text{Un-stained cell count} \times 100}{\text{Total cell count}}$$

Histological Test

After thawing from -80°C, sample B was wrapped with thin porous paper and put in a clearly labeled histological cassette and submerged in 10% buffered formalin. The sample was fixed overnight before it was histologically processed with an automatic tissue processor (Excelsior ES, Thermo Scientific, USA). It was then embedded in paraffin using an embedding center with cryo-console (TEC-2800 HESTION, Amos scientific, Australia). Molten paraffin was poured into histological tray, the sample was removed from cassette and oriented in a cross-sectioning position within the paraffin-filled tray. The tray was immediately cooled to set the paraffin and the tissue embedded inside. The corresponding cassette's lid with its label was placed on top of the tray. The paraffin block was left on cooled surface until the entire block was stable before the tray was removed (Figure 15). The blocks were sectioned into 4-micron thickness using a microtome (Finesse ME+, Thermo Scientific, USA). They were stained with Hematoxylin and Eosin (H&E) and Masson's Trichrome (MTC). Microphotographs were taken from 3 most intact areas of each sample using light microscope (Primo Star, ZEISS, Germany) connected to a digital camera (Canon 550D, Japan) (Figure 16). Thickness of the entire CAM, stromal layer and epithelial layer were measured at 3 randomly selected areas in each microphotograph with a software (Photoshop CC, Adobe, USA). The ratio of epithelial layer to stromal layer (E/S ratio) was calculated by a following equation:

$$E/S \text{ ratio} = \text{Epithelial layer thickness} / \text{Stromal layer thickness}$$



Figure 15: Photographs of (A) CAMs in cassettes fixed in formalin and (B) cassettes with CAMs during embedding to paraffin block.

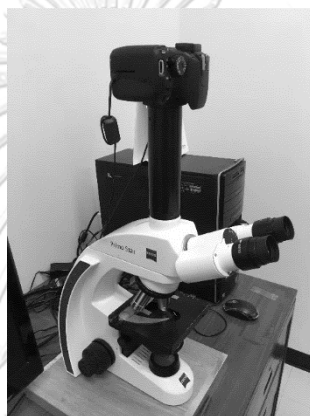


Figure 16: Photograph of microscope connected to a digital camera that was used to take microphotographs of CAM samples.

Data Analysis

Results of tensile strength test parameters (maximum stress, extensibility, Young's modulus, length of toe region, and length of linear region), transparency test parameters (%TTRAN and %Haze), cell viability test (%viable), and histological test parameters (thickness of entire CAM, stromal layer, epithelial layer, and E/S ratio) between 7-d CAM and 30-d CAM were statistically compared by the Mann-Whitney U Test (SPSS version 22; IBM, NY, USA) with a significant level of $p < 0.05$.

Result of sterility test was descriptively reported as either “no growth” or the identification of the bacterial or fungal growth. Anatomical structure and/ or histological changes of CAM were descriptively reported.

CHAPTER 4

RESULTS

Part 1: Biomechanical Properties of Canine Amniotic Membrane

Tensile Strength Test

The stress-strain curve of cryopreserved CAM at 7 and 30 days matched the J-shaped stress-strain curve, which is one of the curves generated from biomaterial. Stress-strain curve of cryopreserved CAMs began with a clear toe region, followed by a steep linear region (Figure 17). Maximum stress was located at the peak of linear region, where the curve abruptly ends at breakage of material.

Among five tensile strength parameters, no parameters were statistically different (Table 1). The median of maximum stress, extensibility, and Young's modulus were higher at day 7, there is no evidence to support a statistical difference between the values (Table 1).

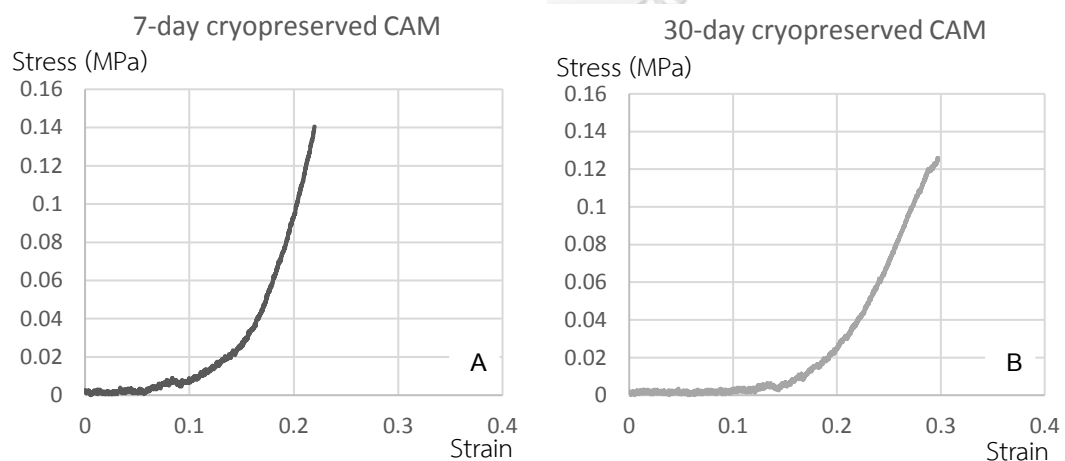


Figure 17: Representative stress-strain curves of (A) 7-d and (B) 30-d canine amniotic membrane. (Note: MPa = Megapascal)

Table 1: Median \pm interquartile range of tensile strength parameters of canine amniotic membranes cryopreserved at 7 and 30 days.

Parameter / Canine amniotic membrane	7 days	30 days
Max stress (MPa)	0.11 \pm 0.10	0.09 \pm 0.05
Extensibility	0.20 \pm 0.15	0.19 \pm 0.07
Young's Modulus (MPa)	0.93 \pm 1.16	0.93 \pm 0.58
Toe region length	0.14 \pm 0.16	0.11 \pm 0.05
Linear region length	0.05 \pm 0.03	0.04 \pm 0.02

Transparency Test

Percentage of TTRAN of the 7-d CAMs and the 30-d CAMs were ranged from 95.21 to 97.79 and 95.13 to 97.86, respectively. Percentage of Haze of the 7-d CAMs and the 30-d CAMs were ranged from 8.91 to 42.91 and 6.23 to 34.17, respectively. Median of percentages of TTRAN and Haze were higher in the 7-d CAM group as compared to the other (Table 2). However, the differences were non-statistical significance.

Table 2: Median \pm interquartile range of transparency parameters of canine amniotic membranes cryopreserved at 7 and 30 days.

Percentage / Canine amniotic membrane	7 days	30 days
Total transmittance	97.14 \pm 0.78	96.89 \pm 0.96
Haze	17.99 \pm 14.17	19.16 \pm 15.08

Part 2: Biological Properties of Canine Amniotic Membrane

Sterility Test

Bacterial culture revealed positive results in 4 samples that were cryopreserved for 7 days (Figure 18); *Staphylococcus* coagulase negative (2), *Pseudomonas* spp. (1) and *Micrococcus* spp. (1). No bacterial growth was observed on the 30-d samples. Four out of 18 sample, cryopreserved for 7 days were positive for fungal culture (Figure 20); *Aspergillus niger* (1), *Fusarium* spp. (1), *Penicillium* spp. (1) and unidentified opportunistic fungi (1). Unidentified yeast (1) was found on the 30-day cryopreserved CAMs.

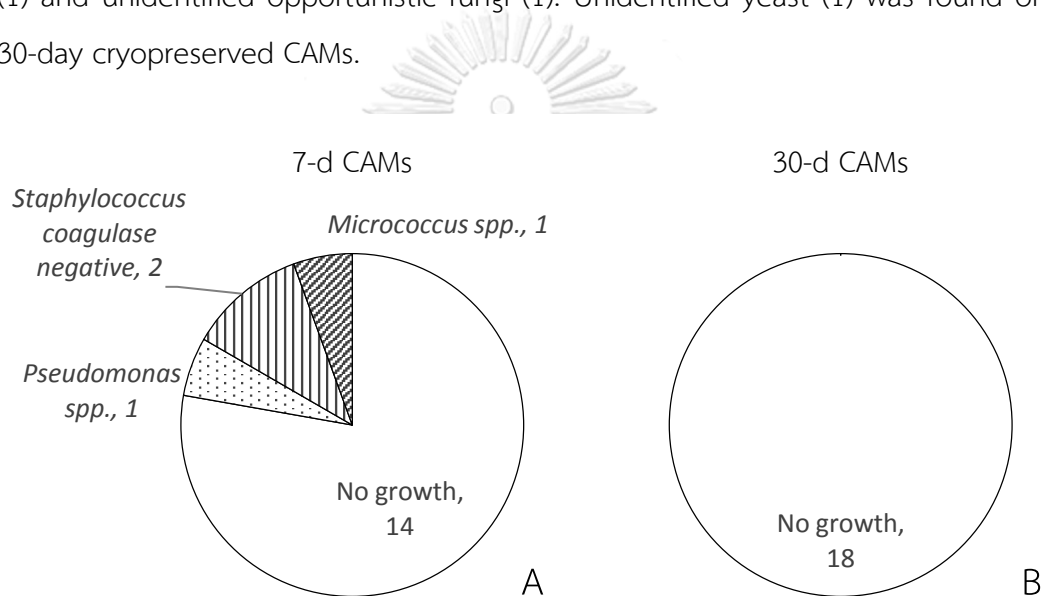


Figure 18 : Pie charts of bacterial culture from (A) 7-d CAM and (B) 30-d CAM samples. (Note that numbers indicate number of positive samples.)

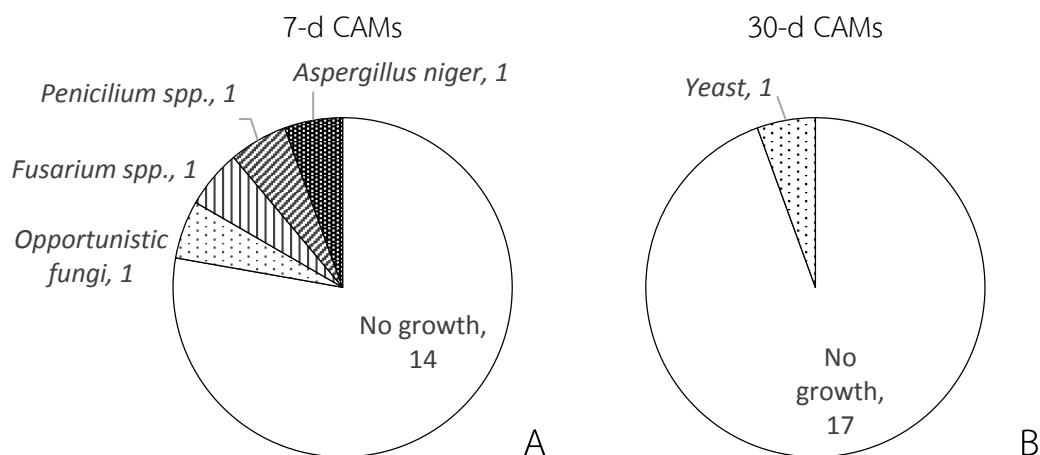


Figure 19: Pie charts of fungal culture from (A) 7-d CAM and (B) 30-d CAM samples. (Note that numbers indicate number of positive samples.)

Cell Viability Test

Sheets of uniformly arranged polygonal epithelial cells that were visible with trypan blue staining represented nonviable cells (Figure 21). The epithelial cells were tightly packed with distinct cell margins. The cytoplasm of stained cells was paler than the nuclei. The cytoplasm of some cells was stained homogeneously while some cells were observed with multiple vacuoles accumulated with Trypan blue. Round eccentric nuclei were more intensely stained than the cytoplasm. Cells without cytoplasmic or nuclei staining represent the viable cells with intact cell membrane. They were sparsely seen scattered among the epithelial cell sheet. Median \pm interquartile range of cell viability percentage of the 7-day CAMs was 8.77 ± 11.39 , while that of the 30-day samples was 1.75 ± 4.70 (Figure 22). By Mann-Whitney U test, cell viability of 7-d CAMs was statistically higher than those of 30-d CAMs.

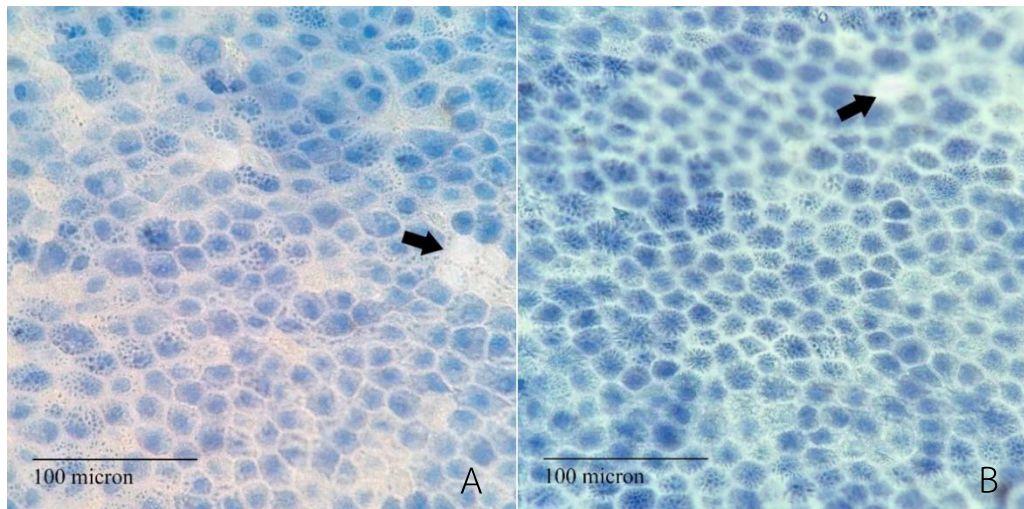


Figure 20: Representative microphotographs showing single layer of epithelium of (A) 7-d CAMs and (B) 30-d CAMs, comprising of nonviable (Trypan blue stained) cells and viable cells (Trypan blue unstained) (arrows). (bar = 100 micron)

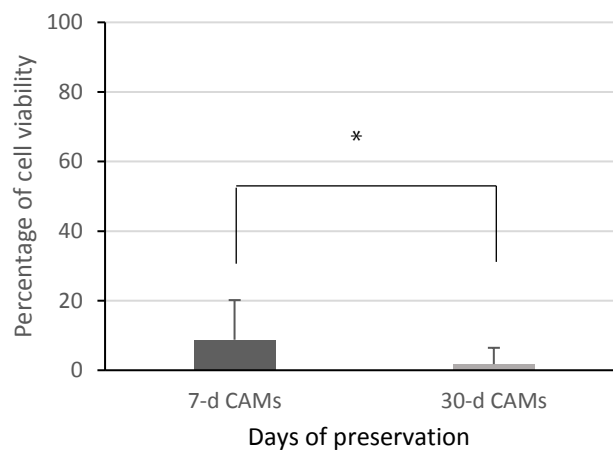


Figure 21: Bar chart of the Median \pm interquartile range of percentage of cell viability of cryopreserved amniotic membranes at 7 and 30 days. Note: Star (*) indicates statistical difference.

Histological Test

Morphology of cryopreserved CAMs showed single-layered epithelial cells with ovoid nucleus. Cilia at the apical surface of the epithelium sloughing off from

the membrane in both groups can be observed. Various epithelial cell morphology was comparably noticed in both groups. Mean epithelial thickness was also statistically comparable (Table 3). The collagen-rich stromal layer was strongly stained with Masson Trichrome (MTC). Two layers of stroma were more clearly observed in 7-d CAM (Figure 23). Collagen fibers in the anterior stroma next to epithelium appeared more compact and regularly arranged when compared to the posterior stroma. Porous structures were observed in the posterior stroma. Active fibroblasts were sparsely observed within the stromal layer in both groups. Median value of overall CAM thickness and stromal layer of 7-d CAM was higher than 30-d CAM. Median values of epithelial layer thickness of both groups were comparable. Median value of E/S ratio of 7-d CAM were lower than of 30-d CAM, which were caused by decreasing of stromal thickness in 30-d CAM. Out of the 4 parameters, only stromal thickness was statistically different (Table 3).

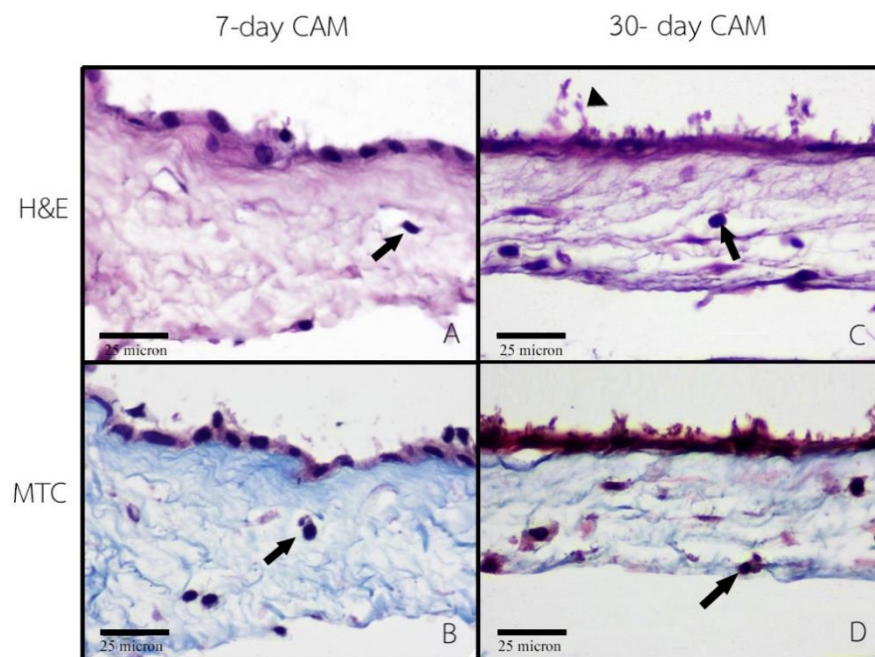


Figure 22: Representative microphotographs of the 7-day canine amniotic membrane stained with (A) Hematoxylin and Eosin (H&E) and (B) Masson Trichrome (MTS), and the 30-day canine amniotic membrane stained with (C) H&E and (D) MTC. Note that arrows indicate fibroblasts within the stromal layer while an arrow head indicates cilia sloughing off from epithelial layer. (magnification power = 400X, bar = 25 micron)

Table 3: Median \pm interquartile range of canine amniotic membranes cryopreserved at 7 and 30 days. Note: Star (*) indicates statistical difference.

Thickness / Canine amniotic membrane	7 days	30 days
CAM thickness (micron)	40 \pm 13	33 \pm 14.75
Epithelial thickness (micron)	7 \pm 2.75	7 \pm 2.75
Stromal thickness (micron)	33 \pm 14.5*	26 \pm 14.75*
Epithelial/Stromal ratio	0.19 \pm 0.09	0.25 \pm 0.09



CHAPTER 5

DISCUSSION

This is the first study of tensile strength and transparency of CAM. The stress-strain curves generated by CAM correspond to the characteristics of J-shaped curve demonstrated in HAM (Chuck et al., 2004), as well as porcine AM (Kikuchi et al., 2016), ovine AM, and equine AM (Borazjani et al., 2011). The J-shaped stress-strain curve is typically found in biological tissues containing collagen and elastin that build up a three-dimensional network such as skin, tendon, and blood vessels (Holzapfel, 2001). All parameters of tensile strength test were lower in 30-d CAMs without statistical significance. This suggests that the duration of cryopreservation may mildly damage cross-linking bond of elastin, resulting in a decrease of its elasticity (Schenke-Layland et al., 2006).

Histological findings of H&E revealed that the stromal layer of AM in humans (Jirsova and Jones, 2017), as well as dogs, cats, rabbits, bovine, and equines (Favaron et al., 2015) is composed of abundant connective tissues. Our histologic results by MTC staining, selectively stains collagen fibers in blue, reveals that CAM majorly contains collagen-rich matrix with fibroblast infiltration. With increasing tensile stress to CAM, representing as a linear region of the stress-strain curve, collagen fibers are straightened completely and arranged themselves parallel to the direction of the applied force. The linear region length of 7-d CAM and 30-d CAM are similar, suggests that collagen fibers are still intact regardless of different duration of cryopreservation.

Porous structure in the posterior part of the stromal layer of CAM resembles histological structure of a spongy layer of HAM (Mamede et al., 2012). This morphology is less distinguishable in samples cryopreserved for 30 days. Glycerol replacing water in CAM (Laranjo, 2015) may have caused more compact arrangement in samples with longer cryopreservation time. Change in structural integrity of 30-d CAM may be related to a decrease of maximum stress, Young's modulus, and

extensibility, since these parameters reflect the structural integrity of collagen fibers in biological materials (Holzapfel, 2001). Such changes are in accordance to the decrease of stromal thickness, which is the layer responsible for the majority of the tensile strength of AM (Riau et al., 2010). Compared to fresh, cryopreserved HAM maintained histological structure as shown by immunohistochemical finding (Rodríguez-Ares et al., 2009). Despite the more compact stromal structure of 30-d CAM, percentage of transparency from 2 groups of cryopreservation were considerably high and comparable. These properties of transparency make CAM a good candidate of biological grafting material for optical purpose of transplantation.

Biomechanical properties of cryopreserved AM were reported in humans and pigs (Tanaka et al., 2012; Kikuchi et al., 2016). Comparison among the three species including dogs, CAM exhibits the least maximum stress, which indicates the least endurance to applied force. It exhibits the least Young's modulus, indicating the lowest stiffness, and it also displays the least extensibility, which refers to the least endurance to deformation. Moreover, CAM is histologically thinner than HAM (Laranjo, 2015). In order to clinically apply CAM for corneal reconstruction in veterinary practice, transplantation of multi-layer suturing technique is recommended to increase tensile strength for tectonic purpose. Using multiple layers of CAM on the canine cornea should not significantly impede optical purpose of the recipient due to its high transparency. Also, cross-linking technique may be additionally be applied to create a resilient and transparent CAM as it was successfully performed with 8 layers of HAM with satisfactory clinical results on experimental rabbits (Tanaka et al., 2012).

At the beginning of the study, contamination with environmental microorganism were found. We speculated that it was because of insufficient sterilization of collection vials. After considering more intensive sterilization process for the collection vials by using a new batch of double layered sterilization wrap, contamination discontinued. There was no relation of number of contaminations between the two groups of experiment. Cryopreservation is not a sterilizing process

(Laranjo, 2015). HAM that were collected by either cesarean section or vaginal delivery can be contaminated (Addis et al., 2001). Collection of AM by cesarean section, however, decreases chance of contamination (Addis et al., 2001). Therefore, aseptic technique must be strictly monitored in every steps of procedures. To reduce chance of infection to patient, random microbial culture from all batches is recommended in a practical setting. As it is a protocol in HAM collection for clinical use (Qureshi et al., 2010)

Low percentage of cell viability of both groups of CAMs, shown by trypan blue uptake of cytoplasm, may indicate increased cell membrane damage from ice crystal formation, which may occur in rapid cooling process (von Bomhard et al., 2016). The finding corresponds to a sloughing off cilia in the epithelial layer as seen in histological study. The use of glycerol as preservation media may be another factor causing epithelial cell damage from change of cell osmolarity (von Bomhard et al., 2016). Cryopreservation with the use of Dimethyl Sulfoxide (DMSO), instead of glycerol, can maintain up to 50% of all viability up to 2 months (Laranjo, 2015). This apparent low cell viability is, however, desirable for the clinical application of CAM for corneal reconstruction. HAM with lower cell viability is preferable in clinical practice (Laranjo, 2015) because of a decrease of inflammatory responses and reduced graft rejection.

This is the first study of biomechanical and biological properties of cryopreserved CAM, we have provided the first data for further study to develop this promising material to be a more effective corneal transplant within the context of veterinary surgery. There were some limitations of this study regarding CAM's thickness, as the anatomical location of CAM and breed of dog were not strictly controlled factors. There are several reports of HAM thickness variation among individuals and anatomical location (Favaron et al., 2015). The heterogenous nature of CAM was taken into consideration during this study's sample collection by selecting similar areas, as the umbilical cord area was generally avoided due to vasculature. However, because of individual CAM's blood vessel location are

different, it was impossible to choose the exact same location of all CAM samples. Moreover, there are no study of breed of dog's effect on CAM's thickness at the time of this study. Effect of longer cryopreservation time might be an interesting further study as the cryopreserved HAM are proven to be effective transplant material after being kept for 6 months (Qureshi et al., 2010).

Conclusion

We have investigated biomechanical and biological properties of the 7-d CAM and 30-d CAM. Biomechanical properties of CAM preserved up to 30 days are comparable to that of 7 days, while there were some differences in biological properties, namely, cell viability of 7-d CAM was statistically higher than 30-d CAM, and stromal thickness of 7-d CAM was higher than 30-d CAM. Cryopreserved CAM is therefore a promising biological material for corneal transplantation with satisfactory characteristics. Multiple-layer corneal transplantation technique for corneal reconstruction is recommended for optical and tectonic purposes in companion animals.

Suggestions

Investigation of other factors, such as breed of dog, preservation methods, and longer cryopreservation duration would provide beneficial information for clinical application.

REFERENCES

- Adds PJ, Hunt C and Hartley S 2001. Bacterial contamination of amniotic membrane. *Br J Ophthalmol.* 85(2): 228-230.
- Aralla M, Gropetti D, Caldarini L, Cremonesi F and Arrighi S 2013. Morphological evaluation of the placenta and fetal membranes during canine pregnancy from early implantation to term. *Res Vet Sci.* 95(1): 15-22.
- Ashraf NN, Siyal NA, Sultan S and Adhi MI 2015. Comparison of efficacy of storage of amniotic membrane at -20 and -80 degrees centigrade. *J Coll Physici.* 25(4): 264-267.
- Barachetti L, Giudice C and Mortellaro CM 2010. Amniotic membrane transplantation for the treatment of feline corneal sequestrum: pilot study. *Vet Ophthalmol.* 13(5): 326-330.
- Barequet IS, Habet-Wilner Z, Keller N, Smollan G, Ziv H, Belkin M and Rosner M 2008. Effect of Amniotic Membrane Transplantation on the Healing of Bacterial Keratitis. *Invest Ophthalmol Vis Sci.* 49(1): 163-167.
- Barros PS, Safatle A, Godoy CA, Souza MS, Barros LF and Brooks DE 2005. Amniotic membrane transplantation for the reconstruction of the ocular surface in three cases. *Vet Ophthalmol.* 8(3): 189-192.
- Berguiga M, Mameletzi E, Nicolas M, Rivier D and Majo F 2013. Long-term follow-up of multilayer amniotic membrane transplantation (MLAMT) for non-traumatic corneal perforations or deep ulcers with descemetocoele. *Klin Monbl Augenheilkd.* 230(4): 413-418.
- Berthaume MA 2016. Food mechanical properties and dietary ecology. *Am J Phys Anthropol.* 159: 79-104.
- Borazjani A, Weed BC, Patnaik SS, Feugang JM, Christiansen D, Elder SH, Ryan PL and Liao J 2011. A comparative biomechanical analysis of term fetal membranes in human and domestic species. *Am J Obstet Gynecol.* 204(4): 365.e025-365.e036.
- Brikshavana P and Kanchanachaya T 2010. Multilayer Human Amniotic Membrane Transplantation for Reconstruction of Corneal Perforation in Dogs. *Thai J Vet*

Med. 132.

- Bussieres M, Krohne SG, Stiles J and Townsend WM 2004. The use of porcine small intestinal submucosa for the repair of full-thickness corneal defects in dogs, cats and horses. *Vet Ophthalmol.* 7(5): 352-359.
- Chuck RS, Graff JM, Bryant MR and Sweet PM 2004. Biomechanical Characterization of Human Amniotic Membrane Preparations for Ocular Surface Reconstruction. *Ophthalmic Res.* 36(6): 341-348.
- Connon CJ, Douth J, Chen B, Hopkinson A, Mehta JS, Nakamura T, Kinoshita S and Meek KM 2010. The variation in transparency of amniotic membrane used in ocular surface regeneration. *Br J Ophthalmol.* 94(8): 1057-1061.
- Davis AM, Riggs CM and Chow DWY 2017. The use of porcine urinary bladder matrix (UBM) to repair a perforated corneal ulcer with iris prolapse in a horse. *Equine Vet Educ.* 31(4): 172-178.
- Dekaris I, Mravicic I, Barisic A, Draca N and Pauk M 2010. Amniotic membrane transplantation in the treatment of persistent epithelial defect on the corneal graft. *Coll Antropol.* 34(2): 15-19.
- Dua HS, Gomes JA, King AJ and Maharajan VS 2004. The amniotic membrane in ophthalmology. *Surv Ophthalmol.* 49(1): 51-77.
- Duchesne B, Tahi H and Galand A 2001. Use of human fibrin glue and amniotic membrane transplant in corneal perforation. *Cornea.* 20(2): 230-232.
- Dulaurent T, Azoulay T, Gouille F, Dulaurent A, Mentek M, Peiffer RL and Isard P-F 2014. Use of bovine pericardium (Tutopatch®) graft for surgical repair of deep melting corneal ulcers in dogs and corneal sequestra in cats. *Vet Ophthalmol.* 17(2): 91-99.
- Espana EM, Grueterich M, Sandoval H, Solomon A, Alfonso E, Karp CL, Fantes F and Tseng SC 2003. Amniotic membrane transplantation for bullous keratopathy in eyes with poor visual potential. *J Cataract Refract Surg.* 29(2): 279-284.
- Espana EM, Prabhasawat P, Grueterich M, Solomon A and Tseng SC 2002. Amniotic membrane transplantation for reconstruction after excision of large ocular surface neoplasias. *Br J Ophthalmol.* 86(6): 640-645.
- Favaron P, Carvalho R, Borghesi J, Anunciação A and Miglino M 2015. The amniotic

- membrane: development and potential applications—a review. *Reprod Domest Anim.* 50(6): 881-892.
- Fukuda K, Chikama T-i, Nakamura M and Nishida T 1999. Differential distribution of subchains of the basement membrane components type IV collagen and laminin among the amniotic membrane, cornea, and conjunctiva. *Cornea.* 18(1): 73-79.
- Gonzalez-Andrades M, Argüeso P and Gipson I 2019. Corneal Anatomy. In: *Corneal Regeneration.* Jorge L (ed). Switzerland: Springer. 3-12.
- Groth A, Maggs D, Miller P and Ofri R 2015. *Slatter's fundamentals of veterinary ophthalmology.* 5 ed. In: Saunders. 520.
- Hao Y, Ma DH-K, Hwang DG, Kim W-S and Zhang F 2000. Identification of Antiangiogenic and Antiinflammatory Proteins in Human Amniotic Membrane. *Cornea.* 19(3): 348-352.
- Hariya T, Tanaka Y, Yokokura S and Nakazawa T 2016. Transparent, resilient human amniotic membrane laminates for corneal transplantation. *Biomaterials.* 101: 76-85.
- Hennerbichler S, Reichl B, Pleiner D, Gabriel C, Eibl J and Redl H 2007. The influence of various storage conditions on cell viability in amniotic membrane. *Cell Tissue Bank.* 8(1): 1-8.
- Holzapfel GA 2001. Biomechanics of soft tissue. In: *The handbook of materials behavior models.* San Diego: Academic Press. 1049-1063.
- Iranpour S, Mahdavi-Shahri N, Miri R, Hasanzadeh H, Bidkhori HR, Naderi-Meshkin H, Zahabi E and Matin MM 2018. Supportive properties of basement membrane layer of human amniotic membrane enable development of tissue engineering applications. *Cell Tissue Bank.* 19(3): 357-371.
- Jirsova K and Jones GLA 2017. Amniotic membrane in ophthalmology: properties, preparation, storage and indications for grafting—a review. *Cell Tissue Bank.* 18(2): 193-204.
- John T 2003. Human amniotic membrane transplantation: past, present, and future. *Ophthalmol Clin North Am.* 16(1): 43-65.
- Kalpravidh M, Tuntivanich P, Vongsakul S and Sirivaidyapong S 2009. Canine amniotic

- membrane transplantation for corneal reconstruction after the excision of dermoids in dogs. *Vet Res Commun.* 33(8): 1003-1012.
- Kikuchi M, Feng Z, Kosawada T, Sato D, Nakamura T and Umezu M 2016. Stress relaxation and stress-strain characteristics of porcine amniotic membrane. *Bio-Med Mater Eng.* 27(6): 603-611.
- Kim JY, Choi YM, Jeong SW and Williams DL 2009. Effect of bovine freeze-dried amniotic membrane (Amnisite-BA) on uncomplicated canine corneal erosion. *Vet Ophthalmol.* 12(1): 36-42.
- Kubo M, Sonoda Y, Muramatsu R and Usui M 2001. Immunogenicity of Human Amniotic Membrane in Experimental Xenotransplantation. *Invest Ophthalmol Vis Sci.* 42(7): 1539-1546.
- Lacerda RP, Peña Gimenez MT, Laguna F, Costa D, Ríos J and Leiva M 2017. Corneal grafting for the treatment of full-thickness corneal defects in dogs: a review of 50 cases. *Vet Ophthalmol.* 20(3): 222-231.
- Lagier J-C, Edouard S, Pagnier I, Mediannikov O, Drancourt M and Raoult D 2015. Current and past strategies for bacterial culture in clinical microbiology. *Clin Microbiol Rev.* 28(1): 208-236.
- Laranjo M 2015. Preservation of Amniotic Membrane. In: *Amniotic Membrane.* Botelho M, Mamede A. (ed). Springer, Dordrecht. 209-230.
- Maggs D, Miller P and Ofri R 2017. *Slatter's fundamentals of veterinary ophthalmology.* 5 ed. In: Elsevier Health Sciences.
- Mamede A, Carvalho M, Abrantes A, Laranjo M, Maia C and Botelho M 2012. Amniotic membrane: from structure and functions to clinical applications. *Cell Tissue Res.* 349(2): 447-458.
- Mao Y, Hoffman T, Singh-Varma A, Duan-Arnold Y, Moorman M, Danilkovitch A and Kohn J 2017. Antimicrobial Peptides Secreted From Human Cryopreserved Viable Amniotic Membrane Contribute to its Antibacterial Activity. *Sci Rep.* 7(1): 13722.
- Marsh KM, Ferng AS, Pilikian T, Desai AA, Avery R, Friedman M, Oliva I, Jokerst C, Schipper D and Khalpey Z 2017. Anti-inflammatory properties of amniotic membrane patch following pericardiectomy for constrictive pericarditis. *J*

- Cardiothorac Surg. 12(1): 6.
- Miglino MA, Ambrosio CE, dos Santos Martins D, Wenceslau CV, Pfarrer C and Leiser R 2006. The carnivore pregnancy: the development of the embryo and fetal membranes. *Theriogenology*. 66(6-7): 1699-1702.
- Mrázová H, Koller J, Kubišová K, Fujeríková G, Klincová E and Babál P 2016. Comparison of structural changes in skin and amnion tissue grafts for transplantation induced by gamma and electron beam irradiation for sterilization. *Cell Tissue Bank*. 17(2): 255-260.
- Nakamura T, Yoshitani M, Rigby H, Fullwood NJ, Ito W, Inatomi T, Sotozono C, Nakamura T, Shimizu Y and Kinoshita S 2004. Sterilized, freeze-dried amniotic membrane: a useful substrate for ocular surface reconstruction. *Invest Ophthalmol Vis Sci*. 45(1): 93-99.
- Ollivier FJ 2003. Bacterial corneal diseases in dogs and cats. *Clin Tech Small Anim Pract*. 18(3): 193-198.
- Ollivier FJ, Kallberg ME, Plummer CE, Barrie KP, O'Reilly S, Taylor DP, Gelatt KN and Brooks DE 2006. Amniotic membrane transplantation for corneal surface reconstruction after excision of corneolimbic squamous cell carcinomas in nine horses. *Vet Ophthalmol*. 9(6): 404-413.
- Prabhasawat P, Tesavibul N, Prakairunghong N and Booranapong W 2007. Efficacy of amniotic membrane patching for acute chemical and thermal ocular burns. *J Med Assoc Thai*. 90(2): 319-326.
- Qureshi IZ, Fareeha A and Khan WA 2010. Technique for processing and preservation of human amniotic membrane for ocular surface reconstruction. *World Acad Sci Eng Technol*. 69: 763-766.
- Riau AK, Beuerman RW, Lim LS and Mehta JS 2010. Preservation, sterilization and de-epithelialization of human amniotic membrane for use in ocular surface reconstruction. *Biomaterials*. 31(2): 216-225.
- Rihardini LD, Suparman S and Komaratih E 2017. Anti-Inflammation and Anti-Fibrotic Effects of Amniotic Membrane on Post-Trabeculectomy Conjunctiva (Experimental Research on *Oryctolagus cuniculus*). *Ophthalmologica*. 42(2).
- Rodriguez-Ares MT, Tourino R, Lopez-Valladares MJ and Gude F 2004. Multilayer

- amniotic membrane transplantation in the treatment of corneal perforations. *Cornea*. 23(6): 577-583.
- Rodríguez-Ares MT, López-Valladares MJ, Tourino R, Vieites B, Gude F, Silva MT and Couceiro J 2009. Effects of lyophilization on human amniotic membrane. *Acta ophthalmologica*. 87(4): 396-403.
- Schenke-Layland K, Madershahian N, Riemann I, Starcher B, Halbhuber K-J, König K and Stock UA 2006. Impact of cryopreservation on extracellular matrix structures of heart valve leaflets. *Ann Thorac Surg*. 81(3): 918-926.
- Singh R and Chacharkar M 2011. Dried gamma-irradiated amniotic membrane as dressing in burn wound care. *J tissue viability*. 20(2): 49-54.
- Tanaka Y, Kubota A, Yokokura S, Uematsu M, Shi D, Yamato M, Okano T, Quantock AJ and Nishida K 2012. Optical mechanical refinement of human amniotic membrane by dehydration and cross-linking. *J Tissue Eng Regen Med*. 6(9): 731-737.
- Tehrani FA, Ahmadiani A and Niknejad H 2013. The effects of preservation procedures on antibacterial property of amniotic membrane. *Cryobiology*. 67(3): 293-298.
- Thomassen H, Pauklin M, Noelle B, Geerling G, Vetter J, Steven P, Steuhl K-P and Meller D 2011. The effect of long-term storage on the biological and histological properties of cryopreserved amniotic membrane. *Curr Eye Res*. 36(3): 247-255.
- Tseng SC 2007. Evolution of amniotic membrane transplantation. *Clin Exp Ophthalmol*. 35(2): 109-110.
- Tsuzuki K, Yamashita K, Izumisawa Y and Kotani T 2008. Microstructure and glycosaminoglycan ratio of canine cornea after reconstructive transplantation with glycerin-preserved porcine amniotic membranes. *Vet Ophthalmol*. 11(4): 222-227.
- Tuntivanich P and Tuntivanich N 2006. The use of human amniotic membrane for the treatment of descemetocoele in a dog. *J Thai Vet Pract*. 18: 57-66.
- Verbruggen SW, Oyen ML, Phillips AT and Nowlan NC 2017. Function and failure of the fetal membrane: Modelling the mechanics of the chorion and amnion. *PLoS One*. 12(3): e0171588.

- von Bomhard A, Elsässer A, Ritschl LM, Schwarz S and Rotter N 2016. Cryopreservation of Endothelial Cells in Various Cryoprotective Agents and Media - Vitrification versus Slow Freezing Methods. *PloS one*. 11(2): e0149660-e0149660.
- von Versen-Hoeynck F, Steinfeld AP, Becker J, Hermel M, Rath W and Hesselbarth U 2008. Sterilization and preservation influence the biophysical properties of human amnion grafts. *Biologicals*. 36(4): 248-255.
- Vongsakul S, Tuntivanich P, Sirivaidyapong S and Kalpravidh M 2009. Canine amniotic membrane transplantation for ocular surface reconstruction of created deep corneal ulcers in dogs. *Thai J Vet Med*. 39(2): 135-144.
- Wang MX, Gray TB, Park WC, Prabhasawat P, Culbertson W, Forster R, Hanna K and Tseng SC 2001. Reduction in corneal haze and apoptosis by amniotic membrane matrix in excimer laser photoablation in rabbits. *J Cataract Refract Surg*. 27(2): 310-319.
- Wolfel AE, Pederson SL, Cleymaet AM, Hess AM and Freeman KS 2019. Anterior segment parameters in normal dogs using the Pentacam® HR Scheimpflug system. *Vet Ophthalmol*. 1-12.

APPENDIX

This appendix contains raw data of canine amniotic membranes included in this study.

Part 1: General data of included canine amniotic membranes

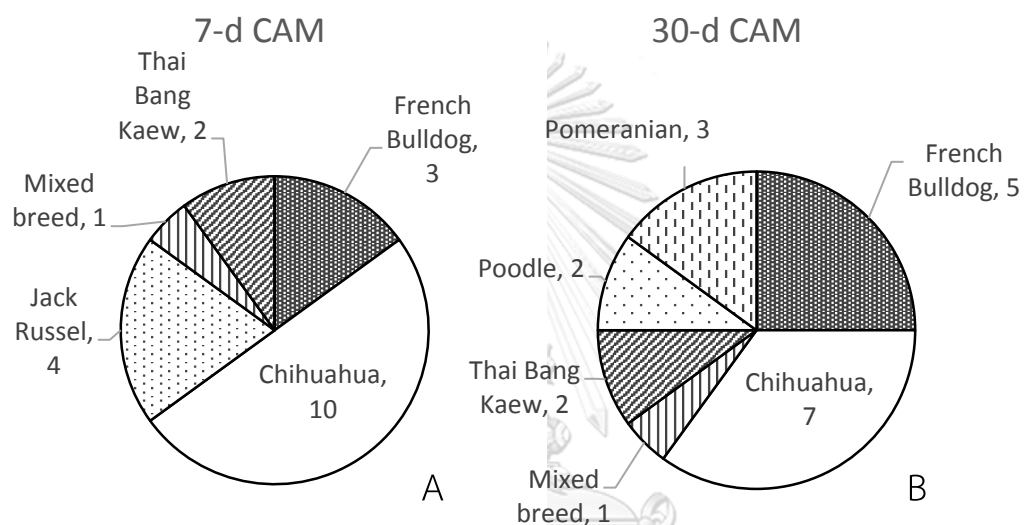


Figure 24: Pie charts of breed of dogs in (A) 7-day and (B) 30-day cryopreserved canine amniotic membrane study groups

Part 2: Biomechanical data of canine amniotic membranes

Table 4: Tensile strength test results of 7-day CAMs

Sample number	Max stress (MPa)	Extensibility (no unit)	Young's Modulus (MPa)	Toe length (no unit)	Elastic length (no unit)
1	0.0515	0.1925	0.4696	0.1200	0.0725
2	0.0523	0.1980	0.5080	0.1275	0.0675
3	0.1995	0.3057	1.6429	0.2575	0.0450
4	0.1350	0.1677	0.5278	0.1150	0.0525
5	0.2105	0.3624	1.4815	0.3100	0.0540

Sample number	Max stress (MPa)	Extensibility (no unit)	Young's Modulus (MPa)	Toe length (no unit)	Elastic length (no unit)
6	0.1938	0.2021	2.4299	0.1650	0.0370
7	0.2190	0.1714	1.0172	0.1430	0.0290
8	0.1548	0.1964	1.5302	0.1433	0.0467
9	0.0888	0.3744	0.8485	0.3150	0.0590
10	0.0707	0.2593	0.5195	0.1960	0.0633
11	0.0855	0.4189	0.4715	0.3350	0.0785
12	0.0820	0.1164	1.4843	0.0925	0.0240
13	0.1292	0.3025	1.7193	0.2483	0.0400
14	0.0823	0.3727	0.6900	0.3067	0.0633
15	0.0445	0.1930	0.4941	0.1225	0.0480
16	0.1525	0.1532	1.8672	0.1063	0.0428
17	0.0345	0.2154	0.1952	0.0900	0.1050
18	0.1435	0.1436	2.2828	0.0850	0.0310

Table 5: Tensile strength test results of 30-day CAMs

Sample number	Max stress (MPa)	Extensibility (no unit)	Young's Modulus (MPa)	Toe length (no unit)	Elastic length (no unit)
1	0.0592	0.1587	0.6966	0.1125	0.0300
2	0.1085	0.2273	0.8258	0.1400	0.0355
3	0.1175	0.2487	1.4674	0.2025	0.0230
4	0.0757	0.1237	1.2792	0.0923	0.0293
5	0.0630	0.1847	0.7696	0.1075	0.0390
6	0.0845	0.1747	0.6714	0.1000	0.0700
7	0.1143	0.2171	1.2290	0.1467	0.0407
8	0.0785	0.1503	0.7125	0.0875	0.0620
9	0.0244	0.2323	0.2121	0.1400	0.0560
10	0.1080	0.1941	0.9075	0.1333	0.0600
11	0.1303	0.1744	1.3335	0.1117	0.0550

Sample number	Max stress (MPa)	Extensibility (no unit)	Young's Modulus (MPa)	Toe length (no unit)	Elastic length (no unit)
12	0.0673	0.1858	0.7467	0.0960	0.0438
13	0.1940	0.1580	2.7895	0.1200	0.0380
14	0.0688	0.0807	1.1722	0.0375	0.0375
15	0.2143	0.2669	1.8976	0.2125	0.0540
16	0.1385	0.2713	1.0871	0.2000	0.0640
17	0.0334	0.0807	0.6160	0.0550	0.0250
18	0.0962	0.1852	0.9500	0.1163	0.0422

Table 6: Transparency test results of 7-day CAMs

Sample number	TTRAN (%)	Haze (%)
1	97.14	20.16
2	97.79	11.84
3	96.65	32.64
4	97.36	15.68
5	96.88	18.98
6	97.54	10.05
7	97.14	17.01
8	97.56	10.27
9	97.66	8.91
10	97.27	13.67
11	96.16	40.11
12	96.8	21.63
13	97.6	9.77
14	97.13	19.43
15	95.21	42.91
16	97.44	10.03
17	95.98	41.3
18	97.02	20.26

Table 7: Transparency test results of 30-day CAMs

Sample number	TTRAN (%)	Haze (%)
1	97.83	6.23
2	95.13	28.63
3	95.8	34.17
4	97.43	11.89
5	97.11	22.18
6	96.76	21.28
7	97.61	7.04
8	97.51	9.7
9	95.87	27.65
10	97.86	7.7
11	96.88	18.9
12	97.27	12.14
13	96.55	26.02
14	97.24	20.25
15	96.31	31.01
16	96.90	18.99
17	96.86	19.32
18	96.88	18.34

Part 3: Biological data of canine amniotic membranes

Table 8: Microbial culture results of 7-day CAMs

Sample number	Bacterial culture	Fungal culture
1	No growth	Opportunistic fungi
2	No growth	<i>Fusarium spp.</i>

Sample number	Bacterial culture	Fungal culture
3	No growth	No growth
4	No growth	No growth
5	No growth	No growth
6	No growth	No growth
7	No growth	No growth
8	<i>Micrococcus spp.</i>	No growth
9	No growth	No growth
10	<i>Pseudomonas spp.</i>	No growth
11	<i>Staphylococcus</i> coagulase negative	<i>Penicillium spp.</i>
12	No growth	<i>Aspergillus niger</i>
13	<i>Staphylococcus</i> coagulase negative	No growth
14	No growth	No growth
15	No growth	No growth
16	No growth	No growth
17	No growth	No growth
18	No growth	No growth

Table 9: Microbial culture results of 30-day CAMs

Sample number	Bacterial culture	Fungal culture
1	No growth	No growth
2	No growth	No growth
3	No growth	Yeast
4	No growth	No growth
5	No growth	No growth
6	No growth	No growth
7	No growth	No growth

Sample number	Bacterial culture	Fungal culture
8	No growth	No growth
9	No growth	No growth
10	No growth	No growth
11	No growth	No growth
12	No growth	No growth
13	No growth	No growth
14	No growth	No growth
15	No growth	No growth
16	No growth	No growth
17	No growth	No growth
18	No growth	No growth

Table 10: Cell viability results of 7-day CAMs

Sample number	Viable cells (%)
1	0.33
2	1.83
3	4.50
4	1.45
5	7.67
6	2.50
7	2.33
8	4.33
9	15.83
10	15.67
11	26.67
12	51.33
13	3.33

Sample number	Viable cells (%)
14	12.00
15	14.80
16	10.97
17	11.12
18	9.87

Table 11: Cell viability results of 30-day CAMs

Sample number	Viable cells (%)
1	0.00
2	1.00
3	2.67
4	0.00
5	1.17
6	1.17
7	1.50
8	6.00
9	1.67
10	1.83
11	0.83
12	26.67
13	19.00
14	16.67
15	1.67
16	5.46
17	4.32
18	6.56

Table 12: Histological measurement results of 7-day CAMs

Sample number	Membrane thickness (micron)	Stroma thickness (micron)	Epithelium thickness (micron)	Stromal /Epithelial ratio
1	86	75	11	0.15
2	76	49	25	0.51
3	58	50	8	0.16
4	35	24	11	0.46
5	30	27	3	0.11
6	36	31	5	0.16
7	20	14	5	0.36
8	30	24	6	0.25
9	35	28	7	0.25
10	49	44	5	0.11
11	59	53	6	0.11
12	45	38	7	0.18
13	36	31	5	0.16
14	36	28	8	0.29
15	34	28	6	0.21
16	44	36	7	0.19
17	45	35	8	0.23
18	44	37	7	0.19

Table 13: Histological measurement results of 30-day CAMs

Sample number	Membrane thickness (micron)	Stroma thickness (micron)	Epithelium thickness (micron)	Stromal /Epithelial ratio
1	16	13	3	0.23
2	53	45	8	0.18
3	45	38	7	0.18

Sample number	Membrane thickness (micron)	Stroma thickness (micron)	Epithelium thickness (micron)	Stromal /Epithelial ratio
4	28	19	9	0.47
5	31	23	8	0.35
6	31	24	7	0.29
7	30	24	6	0.25
8	27	21	6	0.29
9	27	21	6	0.29
10	31	26	5	0.19
11	57	47	10	0.21
12	15	12	3	0.25
13	37	31	6	0.19
14	35	28	7	0.25
15	50	38	12	0.32
16	38	26	12	0.46
17	70	59	11	0.19
18	36	28	7	0.25

VITA

NAME Nathawan Withavatpongton

DATE OF BIRTH 22 January 1990

PLACE OF BIRTH Bangkok

INSTITUTIONS ATTENDED Chulalongkorn University

HOME ADDRESS House No. 70/31, Pracha Uthit Road , Pracha Uthit 113
Alley
Thung Khru Sub-area/Area, Bangkok 10140

PUBLICATION -

AWARD RECEIVED -



จุฬาลงกรณ์มหาวิทยาลัย
CHULALONGKORN UNIVERSITY